An Automated Approach towards Analysing a Good Balanced Horse from a 2D Equine Image

Prateek Tulsyan, B.Tech.

A Dissertation

Presented to the University of Dublin, Trinity College

in partial fulfilment of the requirements for the degree of

Master of Science in Computer Science (Data Science)

Supervisor: Dr. Ciaran Mc Goldrick

September 2020

Declaration

I, the undersigned, declare that this work has not previously been submitted as an exercise for a degree at this, or any other University, and that unless otherwise stated, is my own work.

Prateek Tulsyan

September 12, 2020

Permission to Lend and/or Copy

I, the undersigned, agree that Trinity College Library may lend or copy this thesis upon request.

Prateek Tulsyan

September 12, 2020

Acknowledgments

I would like to express my sincere gratitude to my supervisor, Dr. Ciaran Mc Goldrick for his constant support, attention, and advice while working on this dissertation. With his expertise in Image Processing and knowledge about Horse Conformation, I was able to complete the dissertation.

I would also like to thank my second reader, Prof. Siobhan Clarke for her valuable feedback and suggestions on improving the thesis during the presentation.

Finally, I would also like to thank my wife, Purva, and my parents for supporting me and all my decisions in life.

Prateek Tulsyan

University of Dublin, Trinity College
September 2020

An Automated Approach towards Analysing a Good Balanced Horse from a 2D Equine Image

Prateek Tulsyan, Master of Science in Computer Science

University of Dublin, Trinity College, 2020

Supervisor: Dr. Ciaran Mc Goldrick

The calculation of conformation traits by a horse breeder is an important part of selection before buying any breeding stallion or purchasing a racing horse. These conformation traits involve calculating joint angles and body length ratio, thus giving a measure of the health and performance. The lack of studies available for automatic calculation of conformation traits of a horse motivates building a piece of software which takes in a 2D equine image as input and provides the quality of the horse, thus reducing the need to pay an expert and ascertaining whether or not the horse was worth buying. Since, evaluation of front, back, and top of the horse were not possible using the 2D equine image, the research focuses on evaluating Good Balance: Body Length Ratio (11 traits) and Angular Proportions (12 traits). The process involves four steps: Foreground Extraction, Colour and Texture Analysis, Contour and Corner Detection and Novel Algorithm to detect the Points of Interest and calculate proportions, angles and slopes using these points to determine the quality of the horse. The conformation trait obtained were rated based on the learning from the conformation documents. The result showed slight displacement in Point of Interest around the hip and hind leg region in a few images. With the availability of large labelled dataset from a horse breeder, the work could be carried forward to use CNN technique to plot Points of Interest.

Contents

Acknowledgments **iii**

Abstract **iv**

List of Tables **viii**

List of Figures **ix**

Chapter 1 Introduction **1**

1.1 Motivation 5

1.2 Research Objective 6

1.3 Dissertation Overview 6

1.4 Dissertation Structure 8

Chapter 2 State of the Art **9**

2.1 Importance of Conformation 9

2.2 Traditional Approach 10

2.2.1 Challenges in Traditional Approach 12

2.3 Techniques Studied to Address Challenges in Traditional Approach . . 12

Chapter 3 Research Methodology **17**

3.1 Overview 17

3.2 Architecture 19

3.3 Workflow 21

3.3.1 Image Pre-processing 21

3.3.2 Foreground Extraction 21

3.3.2.1 Approach that gave Good Results? 21
3.3.2.1.1 Instance Segmentation 21
3.3.2.1.2 Colour Segmentation 22
3.3.2.1.3 Horse Extraction 24
3.3.2.2 Approach that gave Poor Results? 25
3.3.2.2.1 Object Detection 25
3.3.2.2.2 Horse Extraction 25
3.3.3 Denoising 26
3.3.4 Colour and Texture Analysis 27
3.3.5 Contour Detection 31
3.3.5.1 Approach that gave Good Results? 31
3.3.5.2 Approach that gave Poor Results? 32
3.3.6 Corner Detection 33
3.3.7 Novel Algorithm to Detect Key Points of Interest 35
3.3.7.1 Extreme Points Detection 35
3.3.7.2 Image Flipping 36
3.3.7.3 Key Points of Interest Detection 36

Chapter 4 Horse Conformation Evaluation **38**
4.1 Body Length Proportion 38
4.1.1 Trait: Body Shape 39
4.1.2 Trait: Body Direction 39
4.1.3 Trait: Body Capacity 40
4.1.4 Trait: Ratio of Length of Top and Bottom Neck 41
4.1.5 Trait: Distance from Poll to Throatlatch and Poll to Muzzle . . 42
4.1.6 Trait: Length of Neck 43
4.1.7 Trait: Wither and Hip Height from Ground 45
4.2 Angular Proportions 45

Chapter 5 Results and Discussion **49**
5.1 Evaluation 49
5.1.1 Conformation Scoring 49

5.1.2 Visual Verification of Hip region points using Colour and Texture Analysis 50
5.2 System Verification 51
5.3 Limitation 53
5.3.1 Stance and Shape of the Horse 53
5.3.2 Colour of the Horse 54

Chapter 6 Conclusion and Future Work **56**
6.1 Conclusion 56
6.2 Future Work 57

Bibliography **58**

Appendices **65**

List of Tables

1.1 Conformation Traits (Angular Proportions) Measured for a Good Balanced Horse. Here **x, y, centre** denotes the three points and **centre** is the point of intersection of these points for which the angle is calculated for. 3

1.2 Conformation Traits (Body Length Ratio) Measured for a Good Balanced Horse. The conditions tab indicate the measurements based on which the conformation scoring is done. 4

4.1 The result obtained after calculating the structural angles. The source of the range of angles (Min and Max) is [5]. The table depicts that most of the structural angles of the horse lies in the ideal range thus giving a confidence for the ideal balance of the horse. 48

List of Figures

1.1 Points of Horse Conformation. Image Source: [9] 2

2.1 The left image shows the scaled and aligned configuration of 44 horse and the right image shows the mean of the same. Image Source: [17] . 10
2.2 The extracted shape of horse and points selected. **(a)** shows the extracted and denoised image from the original image. **(b)** shows the outline of the horse obtained. **(c)** the blue dot shows all the corner points detected and the red dot shows the key points selected manually. Image Source: [6] 12
2.3 The image in the left (object detection) shows a box drawn around the individual objects whereas the image in the right (instance segmentation) determines which pixels belong to each object. Image Source: [40] 13
2.4 An example illustration of both object detection with boundaries and instance segmentation with opacity 0.5. The text on the top of each object shows the type and confidence score of each detected object. Image Source: [21] 14
2.5 A comparison of the HED model prediction with respect to the traditional Canny Edge Detector. **(a)** & **(b)** shows the original image and ground truth respectively. **(c), (d), (e), (f)** shows the output for HED model for different threshold. **(g), (h), (i)** shows the output for Canny Edge Detector for different threshold. Image Source: [23] 15

3.1 Points of Interest of the horse analysed. 18
3.2 An example of what proportions mean. The ration of the white topline to the underline is 2:1. Image Source: [3] 18

3.3 Architecture of the Horse Conformation Analysis 20
3.4 Instance Segmentation of the horse. **(a)** is the resized image input image. **(b)** shows the detected horse via a rectangular bounding box and the label on top of the same indicates the *confidence score = 1.0* of the detected horse. **(c)** Output image: shows the pixel wise separation of the horse image from the background. 22
3.5 Separation of Instance segmented horse image into **(a)** RGB Colour Space and **(b)** HSV Colour Space. 23
3.6 Image segmentation using Colour Spaces. **(a)** is the input image. **(b)** & **(c)** are the range of light and dark pink colours generated from the HSV colour space of input image. **(d)** is the output image obtained by thresholding the range of colours from the input image. 23
3.7 A comparison of methods for performing foreground extraction. **(f)** clearly shows that the output of Grabcut algorithm is higher in quality then compared to other algorithms. Image Source: [57] 24
3.8 Foreground extraction of horse using mask approximation. **(a)** is the resized image from which the horse needs to be extracted. **(b)** is the approximate mask generated for the horse. **(c)** is the output image. . . 25
3.9 Foreground extraction of horse using bounding box approximation. **(a)** is the resized image from which the horse needs to be extracted. **(b)** provides the rectangular coordinates for the detected horse (50, 40, 750, 560). **(c)** is the poorly extracted output image. 25
3.10 Median Filtering Technique. Image Source: [60] 26
3.11 Denoising of the horse image. **(a)** is the foreground extracted horse image. **(b)** is the output received after applying median filtering. . . . 27
3.12 Colour Analysis over horse image for analysing visual verification for angular proportions using Kmeans clustering. **(a), (b), (c), (d)** are the output for (3, 4, 5, 6) clusters respectively. Cluster 5 gives best result and it can be seen in **(c)** that the circles (left, right, bottom) show the change of shade around buttock, hip and stifle joints region respectively. 28
3.13 Calculating the LBP value of the center pixel 4. The first step is to threshold the neighbouring pixels in binary form. Image Source: [25] . 29

3.14 Converting the neighbouring pixels into decimal form to get the LBP value of the center pixel. Image Source: [25] 29
3.15 Texture Analysis over horse image for analysing visual verification for angular proportions using Local Binary Pattern. 30
3.16 Edge Detection using Holistically-Nested Edge Detection CNN model. **(a)** is the denoised horse image. **(b)** is the output image obtained. . . . 32
3.17 Edge Detection performed using Canny Edge Detector Algorithm. **(a)** is the denoised horse image. **(b)** is the poorly edge detected output image obtained. 33
3.18 Corner Detection performed on the Edge detected image. The green dots in the image represents the corners detected. **(a)** is the result obtained after applying Shi-Tomasi Algorithm. **(b)** is the result obtained after applying Harris Corner Detection Algorithm. 34
3.19 The yellow circle around the edge denotes the extreme left, right, top and bottom points. The yellow circle in the center of the horse denotes the center of gravity of the horse. 35
3.20 Image flipping performed to align all the horses to be standing with its head on the right of the image. **(a)** The x-coordinate for the extreme top point in the image is less than half of the width of the image. **(b)** Flipped image. 36
3.21 Detection of key points of interest using the extreme left, right, top, bottom and center of gravity points. The red dots in the image are the key points of interest detected. The blue arrow shows the flow of point detection along the influence of coordinates on selection of a particular point. 37

4.1 **Length from (A) to (D): (190, 197, 172, 166)**. An example illustration of *(Trait: Body Shape)* shows that the length of different body parts calculated are approximately equal to each other A = B = C = D. This depicts that the horse carries equal weight from front to the back. 39

4.2 **Length from (A) to (B): (172, 258)**. An example illustration of *(Trait: Body Direction)* shows that the topline (A) is shorter than the underline (B) and the pink line denotes that the horse is a downhill horse. This depicts that the although the horse has ideal topline to underline ratio but it carries more weight of forehand because it is a downhill horse. 40
4.3 **Length from (A) to (E): (207, 182, 49, 182, 438)**. An example illustration of *(Trait: Body Capacity)* shows that the depth of heart girth (A) is approx. equal to the length from chest floor to fetlock (B), the depth of heart girth (A) is greater than the depth of flank (D) and the height from wither to ground (A+B+C) is equal to length from buttock to shoulder (E). All these ideal conditions depict that the horse has good depth of heart for proper functioning of the vital organs. 41
4.4 **Length from (A) to (B): (217, 98)**. An example illustration of *(Trait: Ratio of Length of Top and Bottom Neck)* shows that the length of topline (A) (measured from poll to wither) is approx. twice the length of the underline (B) (measured from throatlatch to point of shoulder). This depicts that the horse has an ideal range of topline to underline ratio thus, giving the horse an ability to flex at the poll. 42
4.5 **Length from (A) to (B): (103, 181)**. An example illustration of *(Trait: Distance from Poll to Throatlatch and Poll to Muzzle)* shows that the length from Poll to Throatlatch (A) is approx. half the length from poll to the muzzle (B). This depicts that the horse has an ideal ratio of length of throatlatch to the length of head thus, the horse would have proper breathing patter. 43
4.6 **Length from (A) to (D): (181, 227, 595, 234)**. An example illustration of *(Trait: Length of Neck)* shows that the length from Neck (B) (measured from poll to wither) is approximately 1.5 times of length from poll to muzzle, approximately 1/3 times of length of the horse and approximately equal in length from elbow to hoof. This depicts that the horse has an ideal neck length thus giving the horse greater agility and balance. 44

4.7 **Length from (A) to (B): (435, 449)**. An example illustration of *(Trait: Wither and Hip Height from Ground)* shows that the wither height (A) is approximately equal to the hip height from ground (B). This depicts that the horse has proper balance. 45
4.8 **Angle (A): (50°)**. An example illustration of the *(Shoulder slope)* shows that the horse has an approximately ideal angle thus having longer stride and smoothness in its movement. 46
4.9 **Angle (A) to (F): (68°, 59°, 45°, 48°, 72°, 60°)**. An example illustration of the *(Shoulder slope and hip region angles)* shows that the horse would have difficulty in motion due to greater shoulder and back junction slope (B) and point of buttock angle (E). 47
4.10 **Angle (A) to (F): (95°, 73°, 81°, 101°, 72°, 82°)**. An example illustration of the *(structural angles)* shows that the horse would have difficulty in motion due to greater shoulder and back junction slope (B) and point of buttock angle (E). 48

5.1 Visual Verification of Hip region points using Colour and Texture Analysis. **(a) & (b)** is the texture analysis image and it clearly shows the presence of hip, buttock and stifle joints in the circle number 1, 2, 3 respectively. However, texture analysis over horse image appears to be a better visual indicator of the bone structure of the horse. 51
5.2 **(a)** Ideal key points detected of the horse. **(b)** it can be seen that the gap between the hind legs leads to deviation in the detection of points in that region. Another reason is the length of the horse which leads to wrong detection of buttock point. 53
5.3 The result of colour analysis performed over white coloured horse. It does not show any significant finding for the joint angles around hip region. 54

A.1 Example of a Linear Scoring Form 66

B.1 An example illustration of good conformation results obtained irrespective of the colour of the horse. The conformation score for these horses are **(a), (b), (c), (d) : (20/23, 18/23, 18/23, 19/23)**. The difference in the height of the images is because the images were resized using the scale factor set to width = 800. 67
B.2 An example illustration of measure of error displacement if the key point detection of the horse. The conformation score obtained for these horses are **(a), (b), (c), (d) : (21/23, 18/23, 20/23, 19/23)**. The difference in the height of the images is because the images were resized using the scale factor set to width = 800. 68

Chapter 1

Introduction

Conformation is the blueprint of a horse as directed basically by its bone and muscle structures which is not only about having straight legs but also about the length of the bones, the angle of the joints, and the proportions and overall balance of the horse [1]. It involves numerous traits that depict explicit pieces of the body (e.g., head and neck, forehand, chest, back, or rump), the limb morphology (carpal, fetlock, smother, and hawk joints), or the overall proportion (e.g., type and amicability). Traits like the slope of the shoulder and croup, the elbow, carpal, stifle, hock, fetlock joint (pastern) angles, and the shape and angulation of the hoof, is associated with performance, life span and lameness prevalence across different breeds and disciplines [2]. When inspecting horses for conformation, either while thinking about a buy or contending in horse passing judgment on challenges, it is critical to separate things into key standards to abstain from turning out to be overpowered when assembling the general picture. There are five fundamental standards to assess while evaluating a horses conformation: Balance, Structural Correctness, Way of Going, Muscling, and Breed/sex character [3]. Since the later four criteria are not possible to identify from the 2D image, therefore in this study we are going to focus on evaluating the Good Balance: Body Length Ratio (11 traits) and Angular Proportions (12 traits) [4] [5] of a horse. Balance refers to equal distribution of weight from front to back and from top to bottom of a horse and is determined by the bone structure of the horse. It is the most critical aspect and is necessary for movement and performance [3] [6] [7] [8].

An overview of the horse morphology is presented in Figure 1.1 [7] [9] [10] [11] which consists of all the traits that are further used for calculating joint angles and slopes for evaluating horse conformation.

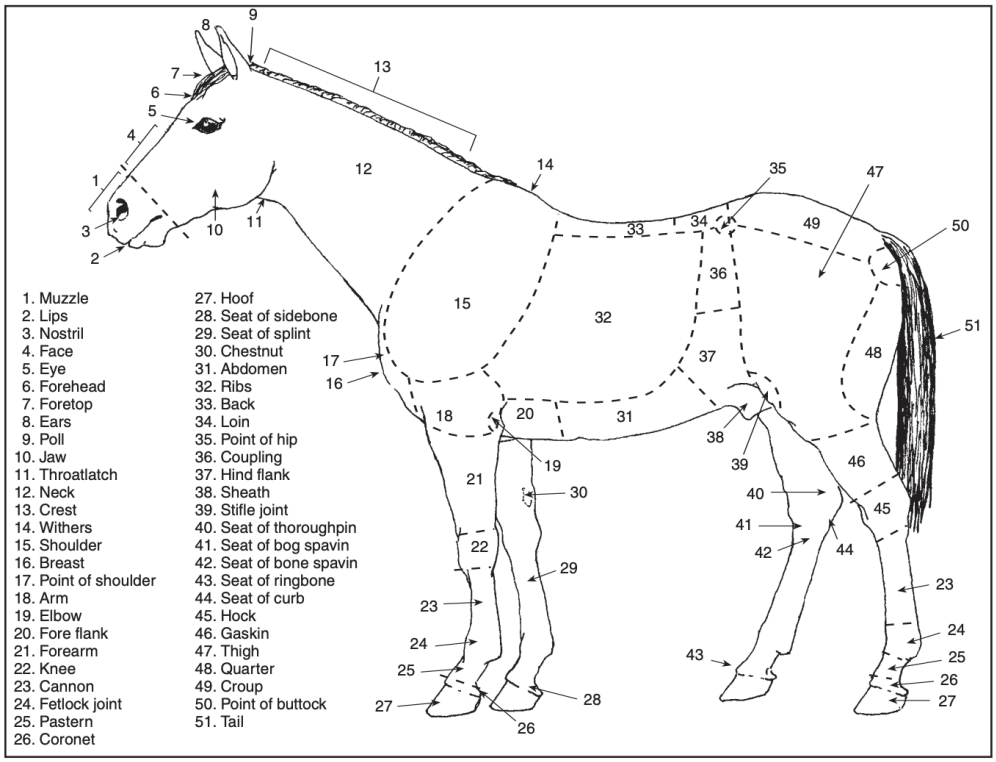

Figure 1.1: Points of Horse Conformation. Image Source: [9]

Based on the study by [3] [4] [6] [7] [8] [11], some conformation traits are hard to be measured using a 2D equine image like hoof angles are difficult to analyse due to grass in the image which leads to improper extraction of hoof area from the image. Traits like hind leg stance are difficult due to tail which leads to improper hind leg outlining and traits from back and front of the horse due to lack of image. Traits like muscle mass are difficult to analyse as it requires viewing the horse from a different angle in order to get the proper shape for muscle. According to [9], a horse when viewed from the front must show a prominent 'V' shape in the front muscling with a large circumference around the forearm. Therefore, in order to analyse and determine whether a horse is Good Balanced, the following conformation traits Angular Proportions (Table 1.1) and Body Length Ratio (Table 1.2) are being measured in the research.

Angle Name	**x**	**centre**	**y**
Shoulder slope	Wither	Shoulder	90° Neck Vertical line
Poll joint	Muzzle	Poll	Top point of wither
Wither joint	Poll	Wither	Point of Shoulder
Shoulder-Elbow Joint	Top point of wither	Shoulder	Elbow joint
Elbow joint	Shoulder	Elbow joint	Cannon
Buttock joint	Hip	Buttock	Stifle
Stifle-Hock joint	Buttock	Stifle	Hock
Stifle-Hip joint	Buttock	Stifle	Hip
Hip joint	Buttock	Hip	Stifle
Wither Upper joint	Shoulder	Peak of Wither	Wither upper point
Wither Lower joint	Shoulder	Peak of Wither	Wither lower point
Shoulder joint	Peak of wither	Shoulder	Shoulder Point Horizontal Straight Line

Table 1.1: Conformation Traits (Angular Proportions) Measured for a Good Balanced Horse. Here **x, y, centre** denotes the three points and **centre** is the point of intersection of these points for which the angle is calculated for.

Conformation Trait	**Condition**
Body Shape	Length of Neck = Shoulder = Back = Hip
Body Direction	Length of TopLine < UnderLine
Body Capacity	Depth of Hearth Girth > Depth of Flank Depth of Hearth Girth = Forearm to Fetlock Wither Height from Ground = Buttock to Shoulder
Length of Top and Bottom Neck Ratio	2*Bottom = Top
Distance from Poll to Throatlatch and Poll to Muzzle	Poll to Throatlatch < Poll to Muzzle
Length of Neck	Length of Neck = 1.5*Poll to Muzzle Length of Neck = 1/3*Length of Horse Length of Neck = Elbow to Hoof
Wither and Hip Height from Ground	Wither Height = Hip Height

Table 1.2: Conformation Traits (Body Length Ratio) Measured for a Good Balanced Horse. The conditions tab indicate the measurements based on which the conformation scoring is done.

The points mentioned in Table 1.2 determines whether a horse is good balanced or not i.e. whether the horse has an equal distribution of weight from front to back, from top to bottom and from side to side. This means that a horse can be light-bodied but also well balanced if it has a proper distribution of bones and proportions for balancing the weight. Proper balance gives the horse more power and smoother movement [3]. The internal body capacity of a horse indicates the space available for the proper functioning of heart and lungs i.e. with more lung capacity, the horse can take in more air after each step making it's movement powerful [9]. The angles such as shoulder slope greatly influence the stride length and smoothness.

1.1 Motivation

With the advancement in the field of image processing and computer vision, few scholars [6] [7] have started using these domains to analyse horse conformation. Both these scholars have used traditional OpenCV [12] Grabcut algorithm [13] directly for extracting horse from the background of a given image. This extraction leads to a change in parameters every time for a different image. They have also used traditional Canny Edge Detection [14] and Harris Corner Detector [15] to initially locate the points and then finally select the key points manually for conformation scoring. These methods again require a change of parameters every time to detect the edge and corners for different images. Few other scholars [16], have used the statistical technique for analysis of shape and equine conformation. The same set of scholars in there next study [17] used image analysis and geometric morphometrics to generate shape-correlated two-dimensional coordinates of the horse to evaluate the conformation. However, most of these research's require some manual intervention or change of parameters between different images. The dearth of research in this field motivates analysing the horse conformation traits automatically and predict the calibre of the horse.

According to [18], the Horse racing industry is expected to be a Billion dollar industry by 2026. The global horse trade industry generates almost $122 billion employing almost 1.74 million people just in the United States which generates almost $79 billion in salaries [19]. This requires a lot of horse breeders to be employed and get proper horse conformation before buying or betting on a horse. A market that is this huge could be targeted to analyse horse conformation automatically within seconds with the use of a mobile application which captures the horse image which is then passed onto the horse conformation scoring model deployed on some cloud service like AWS. This also brings an opportunity to create a product-based application which in future can also be used for analysing the conformation of camels (another huge racing industry in the Arabian Market).

1.2 Research Objective

The *primary objective* of the research is to create a novel algorithm which automatically detects key points located around the edge of the horse for automatic calculation of conformation traits. These key points are detected using the horse's centre of gravity, extreme left, extreme right and extreme bottom point [20].

The *secondary objective* that were also a part of this research are:

1. Automated foreground extraction i.e. segregating horse from the background of the image. The research demonstrates the use of a Deep Learning based pre-trained object detection and mask generating model [21] along with Image Segmentation using colour spaces [22] and then finally extracting the horse using Grabcut algorithm [13].

2. Automated Edge/Contour Detection of the horse. The research here demonstrates the use of a Deep Learning based pre-trained model for Holistically-Nested Edge Detection [23].

3. Another important aspect covered in the research is the use of Colour [24] and Texture Analysis [25] technique on the horse image to determine whether the conformation of joint angles detected show some change in colour or texture around that area.

The research also presents in detail about what techniques or algorithms worked and what did not work during the analysis of the above objectives. The use of pre-trained models was done because of the lack of horse image dataset.

1.3 Dissertation Overview

To achieve the objective of this research, the most popular Artificial Intelligence library OpenCV [12] is used. It is the most popular library used for image processing and solving computer vision problems.

As a first step, the image is first resized to a scale factor set to *width 800* and then passed onto a Deep Learning based pre-trained object detection and mask generating

model [21] for detecting whether the image contains a horse or not and if it does then it generates a mask for the same. The output of this step is then used for image segmentation using the colour spaces [22] generated by the mask. The output generated by the image segmentation and the original resized image is then used passed onto the Grabcut Algorithm [13] to extract the horse from the image.

The output generated by the first step is then Denoised to remove any extra noise from the image for better edge detection. This is achieved using Median Blur algorithm [26]. This denoised image is then used to perform colour analysis using Kmeans clustering technique [24], texture analysis using Local Binary Pattern [25] and Edge Detection using a Deep Learning based pre-trained, Holistically-Nested Edge Detection technique [23].

In the next step, the edge detected image is then used for detecting all the corner points around the edge using Shi-Tomasi Algorithm [27].

The output generated by corner detection is then used to locate extreme left, right, top and bottom points [20]. These extreme points are then used to create a novel algorithm to detect all the key points of horse conformation. Once the key points are located, then they are used to measure different conformation traits which include body length ratio (11) and angular proportions (12).

The measurement of these conformation traits are then used for evaluating whether the horse is Good Balanced or not. The horse is evaluated by giving a +1 score for every conformation trait it has and based on the score, the horse's quality is accessed. Since the calculation of exact length and angle is tricky, therefore a range of $\pm$ 30 pixels is considered for body length ratio and a range of $\pm$ 5° for angular proportions. On evaluation, the horse is rated based one of the three qualities: Poor, Average and Good Balanced.

Finally the entire piece of software was tested on a total of 30 horse images collected from Google Images (5) and *Stallion Selection for Horse Sport Ireland 2019 and earlier (25)* [28].

Apart from above steps, the dissertation also presents what techniques and algorithms did not work or gave an expected result like Rectangular coordinates used for foreground extraction in Grabcut algorithm [13], Gaussian Blur [26] and Bilateral Filter [26] algorithms used for image denoising, Harris Corner algorithm [15] used for corner detection.

1.4 Dissertation Structure

The layout of the dissertation is orchestrated as following:

Chapter 2 State of the Art focuses on studies that have been carried out for analysing horse shape and its conformation along with different conformation scoring techniques.

- First section deals with the studies that tell us about the importance of horse conformation and how it influences the selection of a horse.
- Second section presents the studies that have been carried out so far for the analysis of horse shape and scoring of conformation traits.
- Third section tells us about the challenges faced by the existing research that has been done so far on horse shape analysis.
- The last section presents all the studies that had different research objectives but that have been used as a part of this research.

Chapter 3 Methodology outlines the overall main research methodology. It includes two modules:

- System Design: This section highlights the overall architecture of the software
- Horse Conformation Evaluation: This section evaluates all the conformation traits required for rating the horse as good balanced.

Chapter 4 Results and Discussion outlines the results obtained from the research. It also outlines the limitations of the research and possible solutions for the same.

Chapter 5 Conclusion and Future Work sums up the primary result of this research and proposes manners by which the result can be improved in future.

Chapter 2

State of the Art

This chapter focuses on the related work that has been carried out for analysing horse conformation along with different conformation scoring techniques. The first section explains the importance of horse conformation. The second section explains the studies that have been carried out so far for analysis of horse conformation, conformation scoring techniques, extraction of horse image from the background and different shape analysis methods. This section also provides in detail the challenges faced by these approaches. The last section presents how all the available studies used for different objectives can be used to address the challenges faced in analysis horse conformation. This section also presents use case of colour and texture analysis over a horse image which has mostly been used in the past for forgery detection and pattern recognition.

2.1 Importance of Conformation

A horse's effective performance is closely connected to its conformation. A horse that isn't appropriately conformed for a specific discipline will have lesser chance to succeed in that discipline. This will result in the horse being trained for more number of hours with less satisfactory results. In general, a horse with poor conformation will have more chances of getting an injury along with a tendency towards lameness [29] [30] [31]. There are many opinions on what makes a good horse like, breed, genetics, structure, attitude or training but the most important aspect is conformation which tells how a horse's body part is put together. Even if the horse belongs to the most

popular horse breed, but if it does not have the proper conformation for the discipline it has been selected, then it won't be able to perform [32].

2.2 Traditional Approach

The complications involved with the horse conformation has led to various methods that are being investigated in this domain. Various studies have been conducted, each with different objectives.

In the year 2015, Druml T. and his team members [17] used geometric morphometrics methods by merging with regression analysis to map a rating on the horse image and then analyse the horse shape of 44 Lipizzan mares and further use empirical judgements for the association of conformation traits with the horse image. Through this, they could find the normalized horse shape data which was utilized to further explain the trait influence of horse shape. Figure 2.1 below explains the same.

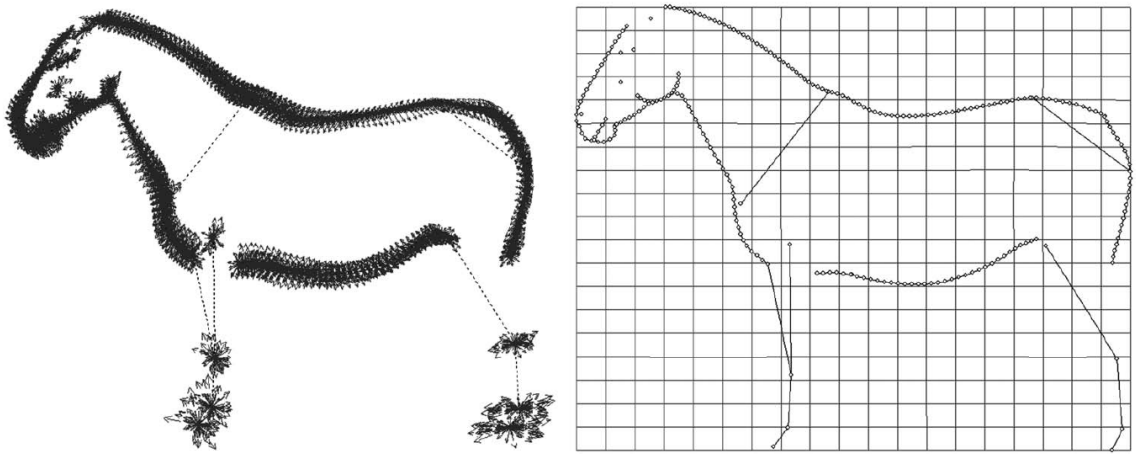

Figure 2.1: The left image shows the scaled and aligned configuration of 44 horse and the right image shows the mean of the same. Image Source: [17]

In the year 2016, Druml T. again with the same set of scholars [16] used the previous horse shape analysis to rate score for 102 Lipizzan horses using eight inter raters. The conformational scoring was based on a valuating scale which is the most commonly used scoring method for Lipizzan horses. Again in the year 2018, Druml T. with another set of scholars [2], studied how genetic background of horses affect the joint angles of

the horse. To improve the evaluation of conformation traits of horses, Druml T. with few other team members [5] in the year 2019, extracted the joint angle of horses using landmark triplets and further assessed the consistency and repeatability of the same using Procrustes analysis. They also introduced another subjective scoring technique to classify the posture of the horse.

Another study by. Thorvaldur K. and his colleagues [33] used statistical analysis on Icelandic horses to study the genetic relationship between the association of different conformation traits and the riding ability of the horse. The results from the study show that a combination of conformation traits used for scoring a horse are better performance indicators than measuring single conformation traits. There was a study done by Hadi G. and his colleagues [34] on Iranian Turkoman Horses which shows how the genetic factors (gene frequency) and non-genetic factors (sex, age and horse management) affect the conformation traits of these horses. The main result obtained from there study was that these factors do affect a horse's conformation and must be considered while evaluating horse conformation trait for a particular discipline like sport, trekking, etc.

While the previous studies are mostly based on a statistical analysis of horse shape, but now, with the advancement in the field of image processing and new computer vision libraries like OpenCV [12], both the Scholars [6] and [7] used these libraries to successfully extract the horse from the image and present an outline of the same for trait analysis using the landmark points. Scholar [6] used the technique of extracting the horse from the image that required a change of parameters for each image. The key points for conformations traits as shown in Figure 1.1 were then calculated manually and then conformation was evaluated by giving a +1 score for each trait that fall in the good range. Figure 2.2 shows the results obtained. However, on the other hand, Scholar [7] provided a manual interface for selecting the rectangular coordinates to extract the horse image. The key points are located from a range of key points previously stored in the database and in case of failure i.e. point misplacement, provides an interface to select the key points manually. The research uses a Linear profiling technique is used to evaluate the conformation, movement and athleticism of the horse which describes where a horse lies between the biological extremes for any given trait [35] [16]. An example of the Linear profiling technique scoring form can be seen in Figure A.1.

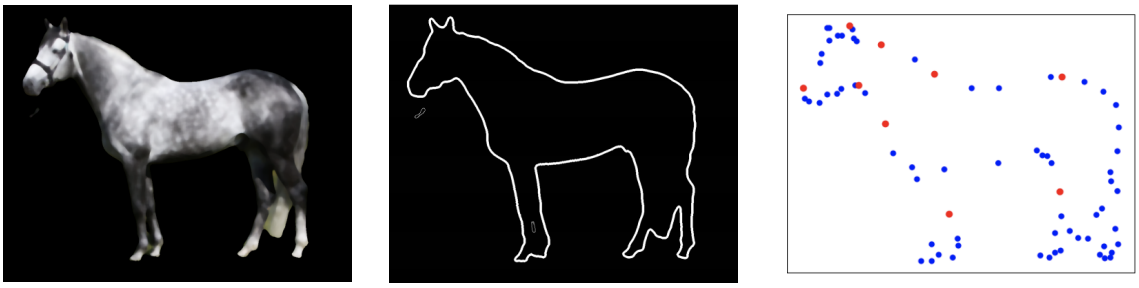

(a) (b) (c)

Figure 2.2: The extracted shape of horse and points selected. **(a)** shows the extracted and denoised image from the original image. **(b)** shows the outline of the horse obtained. **(c)** the blue dot shows all the corner points detected and the red dot shows the key points selected manually. Image Source: [6]

2.2.1 Challenges in Traditional Approach

- **Foreground Extraction:** The extraction of horse from the image requires change of parameters for different image or some sort of manual intervention.
- **Edge Detection:** The outline of the horse detection misses the edge near place between the tail and the hind leg, elbow and forearm region.
- **Corner Detection:** The detection of corner require a change of threshold values between different image.
- **Manual Key Point Selection:** The selection of key points out of all the detected corners needs manual intervention.

2.3 Techniques Studied to Address Challenges in Traditional Approach

In recent years, Deep Learning and Convolutional Neural Networks (CNN) have revolutionized the future of artificial intelligence (AI). It belongs to a broader family of machine learning with the power of representation learning. It has evolved in the field of object detection and recognition, image segmentation and edge detection. The deep learning models are fast, accurate and simple to integrate than the traditional approaches for above-mentioned tasks.

Ross G. with his colleagues [36] [37], combined regional proposals with CNN for object detection (R-CNN). Few Google scholars [38], proposed another very interesting architecture for object detection in the year 2017, called as the MobileNets. This architecture used depthwise separable convolutions for building neural networks. The architecture also provides two parameters for a trade-off between latency and accuracy.

Another study [39] used a custom modified CNN's SegNet architecture for instance segmentation [40] of objects from the image which is segregating the outline of the object from the image and determining which pixel belongs to each object. Figure 2.3 below illustrates the difference between object detection and instance segmentation.

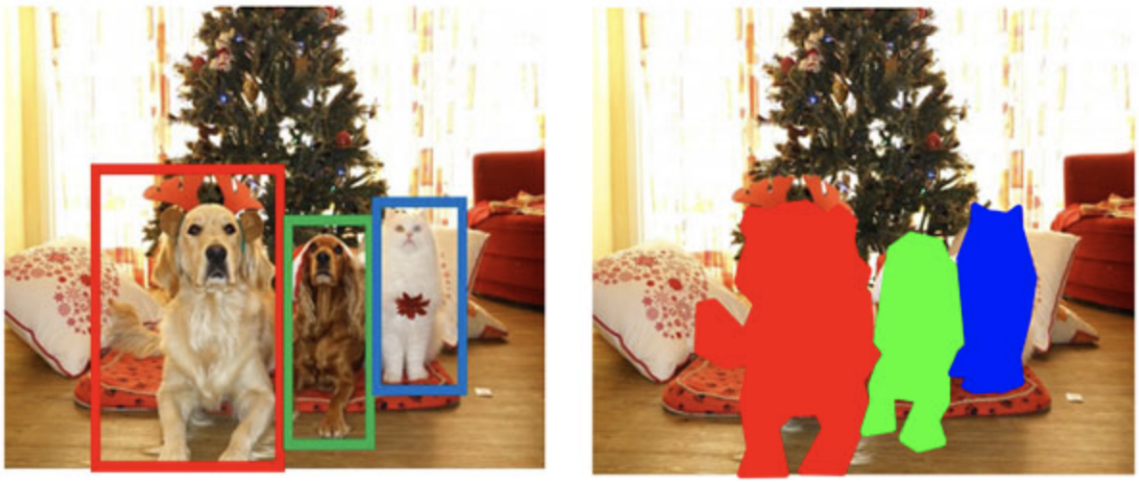

Figure 2.3: The image in the left (object detection) shows a box drawn around the individual objects whereas the image in the right (instance segmentation) determines which pixels belong to each object. Image Source: [40]

A study by Facebook Research team [41] built a deep learning based state-of-the-art architecture for instance segmentation with a feature for changing colours along with the use of opacity function for each colour, called as Detectron. This model has been further used by [21], to obtain both object detection and instance segmentation for an object in an image. The model also detects the type of object along with the confidence score for that object detection i.e. how confident the model is in predicting the type of that object. An example for the same is illustrated in Figure 2.4. This is the model that has been used in the thesis for the first stage of foreground extraction i.e. determining if the image contains a horse and segment if from the rest of the image.

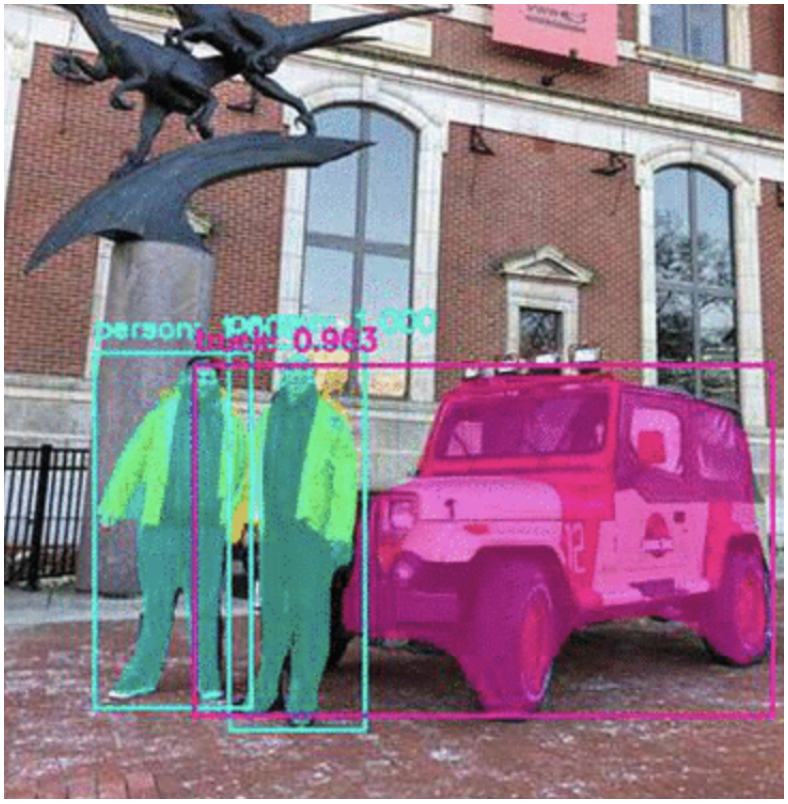

Figure 2.4: An example illustration of both object detection with boundaries and instance segmentation with opacity 0.5. The text on the top of each object shows the type and confidence score of each detected object. Image Source: [21]

The traditional approaches like Canny Edge Detector [14] for edge detection of an object from an image lacks semantic understanding i.e. understanding the content of the image and has limited accuracy. This has been overcome with deep learning architectures. Some of the studies [42] [43] [44] [45] show that deep learning based trained models are able to find more acute and precise edges than pre-existing techniques. One of the deep-learning based methods called as the Holistically-Nested Edge Detection (HED) architecture by Saining X. [46] has now been included in the OpenCV's DNN module for edge detection because it is better than other deep learning models in terms of accuracy and speed, as it uses the side outputs generated by each CNN layer for the prediction. [23] depicts the prediction of HED model as compared to the traditional approach like Canny edge detection. Figure 2.5 shows the different outputs obtained with different thresholds for HED and Canny Edge Detector on the same image.

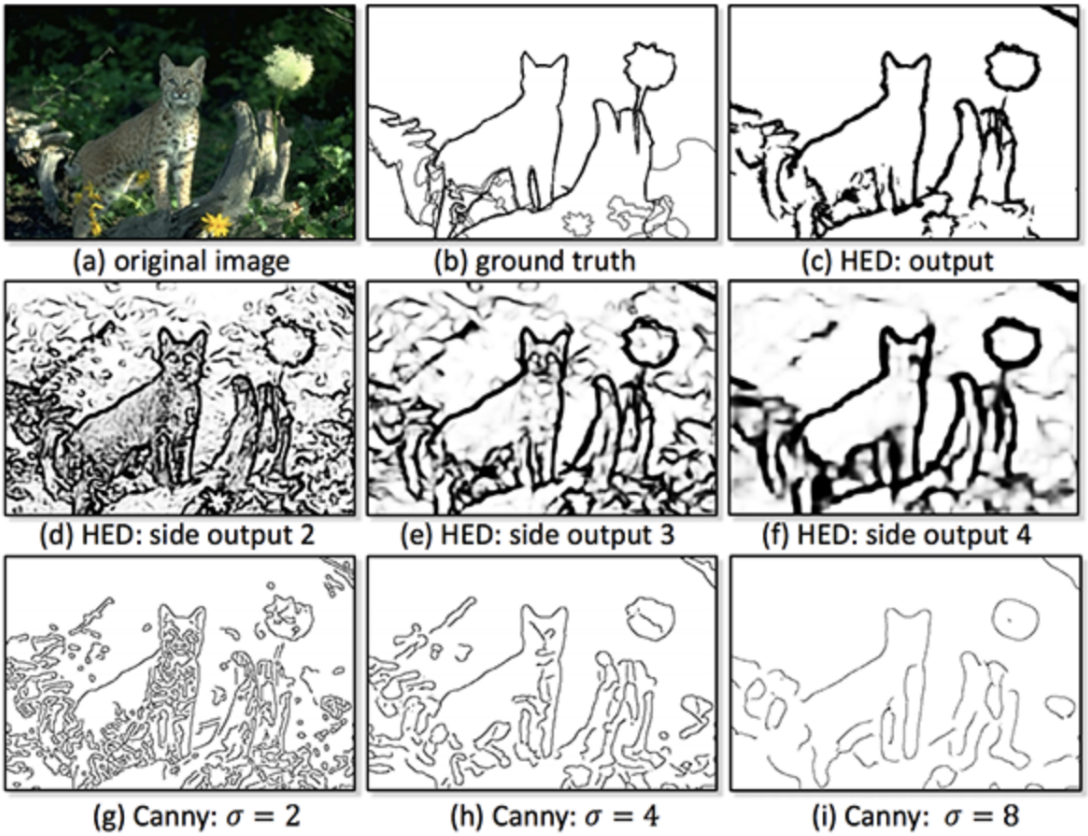

Figure 2.5: A comparison of the HED model prediction with respect to the traditional Canny Edge Detector. **(a)** & **(b)** shows the original image and ground truth respectively. **(c), (d), (e), (f)** shows the output for HED model for different threshold. **(g), (h), (i)** shows the output for Canny Edge Detector for different threshold. Image Source: [23]

All the current research motioned above are based on the analysis of the horse shape from the outline and calculation of traits from those outline points even in the case of joints. But none of the research currently shows if these points which depict the joint angles can be verified by the colour and texture analysis over the horse image as if seen clearly, the horse image clearly shows some darker shade of colour around the joins like the hip region, elbow and forearm region, hock and cannon region in the legs. There are several colour analysis algorithms with the cluster-based colour segmentation technique (Kmeans algorithm) being the most common one. This technique has been previously used in satellite imagery for updating geographical information [47],

analysis of colour spaces of an image [48] and measuring the performance of different colour channels of an image [49]. On the other hand, texture analysis has been used for forgery detection, classification and identification of textures and patterns in images. One such algorithm is Local Binary Pattern [50] [51].

The research above indicates that there is a dearth of study available in the filed of automatic evaluation of horse conformation from a 2D equine image. This provides a source of inspiration to design a system that automatically calculates conformation traits of a horse. The study has been inspired from the previous studies done by [6] [7]. The evaluation of the system is based on the learning developed from the conformation documents [1] [3] [4] [8] [9] [10] [11] . The research also adds the learning developed from [36] [37] [38] [39] [40] [42] [43] [44] [45] [48] [50] in order to better decompose the horse for analysis of conformation traits.

Chapter 3

Research Methodology

The research fabricates onto the work done by Megan R. (2019) [6] and Chun-Hung C. (2019) [7]. Specific parts of the methodology in this examination have been inspired by the decisions these scholars have made. This is on the grounds that their methodology has ended up being a decent beginning advance in tending to the research objective. It also allows for a better comparison of the results. The research addresses the challenges faced by these scholars and introduction of some other new technology that can be used to answer the research objective. Differences in the methodology include the introduction of new foreground extraction technique, Contour and Corner detection, Colour and Texture Analysis and a Novel algorithm to detect key points around the horse.

3.1 Overview

The research uses 2D images of horses for analysing and calculating the conformation traits of a horse. Analysing and calculating the conformation of each point of the horse as seen in Figure 1.1 is very tricky because of the shape of certain parts of a horse like the hind legs, or the hoof area. This is because it is extremely difficult to extract the hoof of a horse if it is standing on grassy area.

So to avoid the complications that are involved in analysing the conformation traits of a horse, the research is focused on analysing only those traits of a horse which can be used to classify the horse as Good Balanced [3]. Figure 3.1 highlights the same.

These traits are then used to calculate the length of different body parts and the angle of joints. The lengths which are recorded are then used to calculate proportions of a certain trait (as seen in Figure 3.2). These proportions are further used to classify the quality of the horse. This has been done to avoid the problem of comparison of lengths in between images which may arise due to different scale and size of horses in different images.

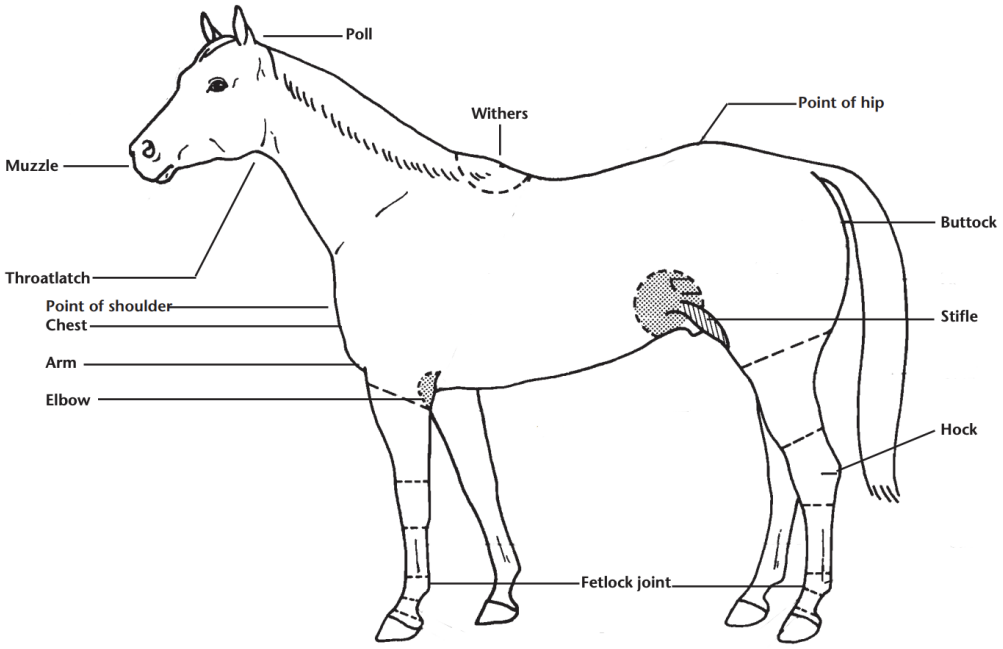

Figure 3.1: Points of Interest of the horse analysed.

Figure 3.2: An example of what proportions mean. The ration of the white topline to the underline is 2:1. Image Source: [3]

3.2 Architecture

The goal of the research is to create a piece of algorithm that can effectively analyse horse conformation and determine the quality of the horse. Figure 3.3 lists down all the steps involved in the process of analysis of horse conformation traits. The images also list down the best algorithm selected for the purpose of that feature. The bottom right part of the figure lists down the icon of all the tools, technologies and libraries used for the purpose of this research.

- **Image pre-processing:** Resize the original image to the scale factor set to width 800.
- **Foreground Extraction:** An algorithm to extract the horse from within the image by removing all the unnecessary background. This process involves three steps: instance segmentation for pixel wise separation of horse image, black and white mask generation and using the resized image and black and white mask generated to extract the horse image.
- **Denoising:** An effective algorithm to remove any extra noise from the extracted image. This smoothens and sharpens the edges of the image.
- **Colour and Texture Analysis:** Perform colour and texture analysis over the foreground extracted image in order to verify visual verification of the calculated joint angles.
- **Contour Detection:** An algorithm to detect the edge from the foreground extracted image and then from that image identify all the corners around the edges.
- **Corner Detection:** An effective algorithm to detect all the corners around the edges of the image.
- **Novel algorithm for Key Point Selection:** An algorithm to detect all the key points for analysis of conformation traits.
- **Balancing aspect Analysis and Conformation Scoring:** Calculation of body length ratio and joint angles for the analysis of different body traits. Finally after scoring these traits the quality of the horse is determined.

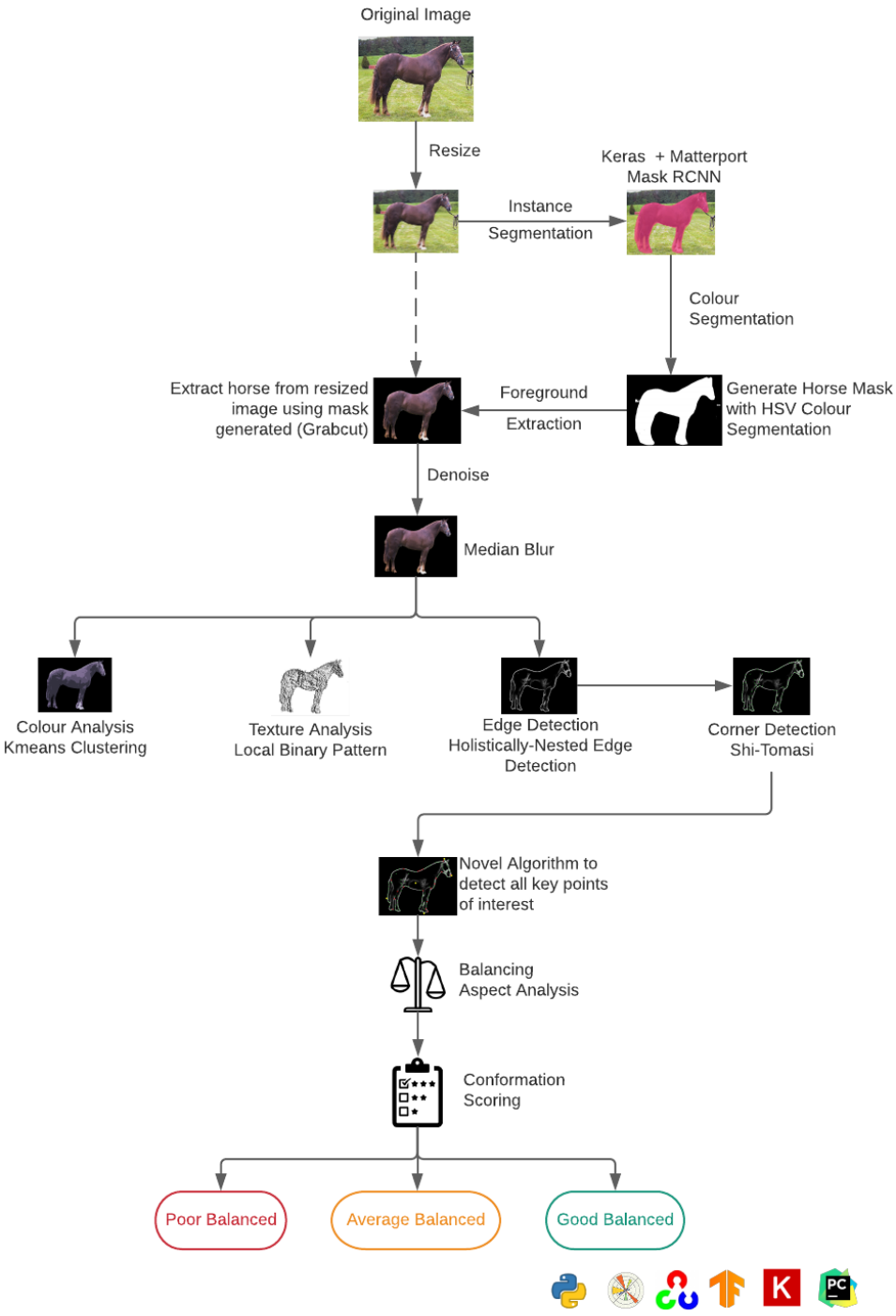

Figure 3.3: Architecture of the Horse Conformation Analysis

3.3 Workflow

This section presents the workflow of the algorithm in detail along with what algorithms or processes worked and gave good results for a particular feature and what algorithms did not give proper results.

3.3.1 Image Pre-processing

As a first step, the image is resized to a scale factor set to width 800. This is being achieved by using OpenCV's *"cv2.resize"* command [12].

3.3.2 Foreground Extraction

This section takes in the resized image from Section 3.3.1 as input and extracts the horse from within the image by removing unnecessary background from the image.

3.3.2.1 Approach that gave Good Results?

3.3.2.1.1 Instance Segmentation

Instance Segmentation is the generation of a pixel wise mask of the object that has been detected in the image [40], thereby segmenting the foreground object from the background. The study uses the Mask R-CNN (Region Based Convolution Network) architecture being proposed by Kaiming H. et al. [41] which has been built on top of previous object detection work being done by Ross G. et al. [52] [53] [54]. The advantage of using Mask R-CNN architecture is that it not only works for object detection but can also perform instance segmentation.

The study uses a Matterport's [55] implementation of Mask R-CNN model is used which is pre-trained on COCO dataset (One of largest object detection and segmentation dataset backed by Facebook) [56] and consists of 80 class labels out of which 1 is horse [21].

To perform instance segmentation the model first detects whether the object detected in the image belongs to class *'horse'* and has a *'confidence score > 0.9'*. The confidence score indicates the confidence the model has in predicting the class of object detected. After this, the model generates the pixel wise mask of the horse detected,

which has been modified to generate a mask larger than the size of the horse for better extraction of the horse image. Figure 3.4 below illustrates the same.

(a) (b) (c)

Figure 3.4: Instance Segmentation of the horse. **(a)** is the resized image input image. **(b)** shows the detected horse via a rectangular bounding box and the label on top of the same indicates the *confidence score = 1.0* of the detected horse. **(c)** Output image: shows the pixel wise separation of the horse image from the background.

3.3.2.1.2 Colour Segmentation

This step involves the segmentation of image using their colour spaces [22] and takes in the image generated in Section 3.3.2.1.1 as input.

The most common colour space is RGB which is represented in terms of red, blue and green components of an image. Another common colour space is HSV (Hue, Saturation, value/luminance) which basically is used for identifying contrast in images. It is the most used colour space in web designing and colour selection tools.

In this process the input image is first separated into RGB and HSV colour space. Figure 3.5 below shows the colour distribution of image pixels in a 3D plot where each axis represents the different channels in the color space. The left image is the separation in RGB colour space and right is the separation in HSV colour space.

It is evident from the Figure 3.5a that the pink part of the image spans over the entire range of RGB values, so it is difficult to separate the pink colour range from the RGB colour space. However, in the Figure 3.5b, the pink colour is more localized and is visually separable. The saturation and value does differ but it located in a small range. By visually analysing the range of pink values across HSV colour space, two colour values are selected, light pink (159, 50, 50) (Figure 3.6b) and dark pink (179, 255, 255) (Figure 3.6c) shown in Figure 3.6b and Figure 3.6c respectively.

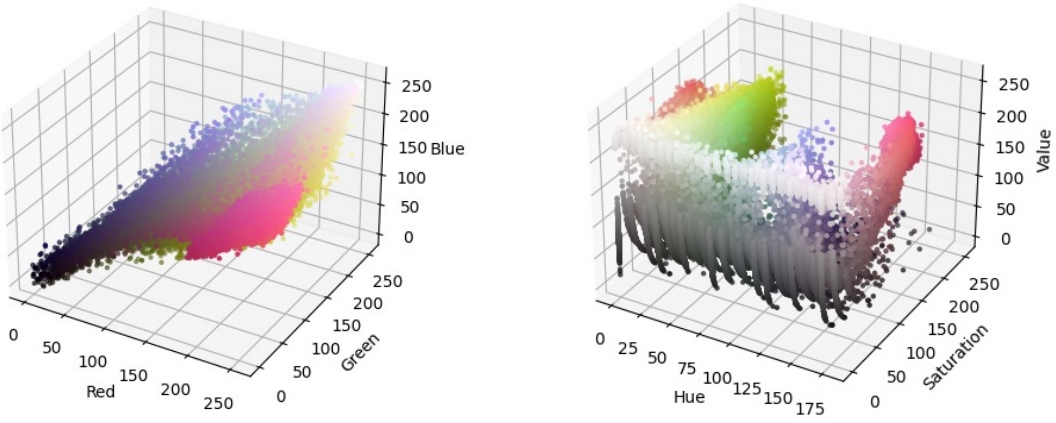

(a) (b)

Figure 3.5: Separation of Instance segmented horse image into **(a)** RGB Colour Space and **(b)** HSV Colour Space.

The range of pink colours found from HSV space are further used as threshold for the input image. The function *'cv2.inRange(input image, lower colour range, upper colour range)'* is used to generate a binary mask (array of 1's and 0's). The value 1 here represents the values within the range of colours selected and 0 represents outside the range. This array is then passed onto the function *'cv2.bitwise_and(input image, input image, binary mask)'*. This function keeps all the pixel values corresponding to 1 and ignores the rest. The 1 values are replaced with white colour and rest with black. Figure 3.6 below shows how the output image (Figure 3.6d) is segmented using the the range of colours light pink (159, 50, 50) (Figure 3.6b) and dark pink (179, 255, 255) (Figure 3.6c) from the input image (Figure 3.6a).

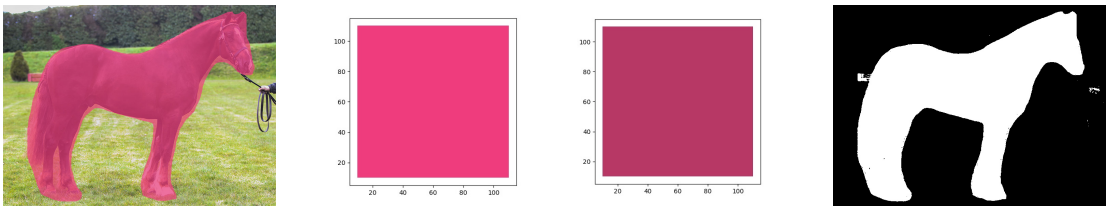

(a) (b) (c) (d)

Figure 3.6: Image segmentation using Colour Spaces. **(a)** is the input image. **(b)** & **(c)** are the range of light and dark pink colours generated from the HSV colour space of input image. **(d)** is the output image obtained by thresholding the range of colours from the input image.

3.3.2.1.3 Horse Extraction

This step involves the extraction of horse image by removing all the unnecessary background from the image. It takes in the resized image from Section 3.3.1 and the output image mask from Section 3.3.2.1.2 as input.

The study uses OpenCV's Grabcut [13] method for foreground segmentation and extraction of the horse image. The reason for selecting Grabcut algorithm for the same is the study provided by Carsten R. et al. [57], which shows a comparison of different algorithms used for foreground extraction. Figure 3.7 below indicates that Grabcut algorithm performed much better than compared to other algorithms.

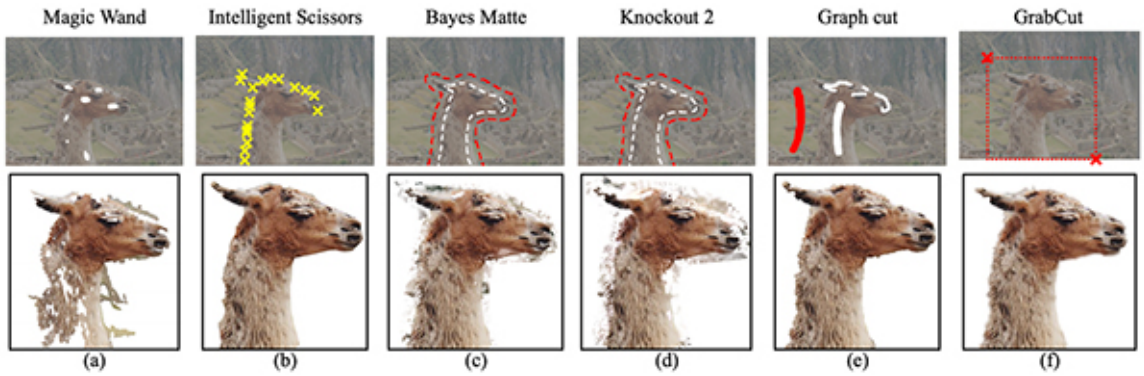

Figure 3.7: A comparison of methods for performing foreground extraction. **(f)** clearly shows that the output of Grabcut algorithm is higher in quality then compared to other algorithms. Image Source: [57]

The Grabcut algorithm provides two approaches for foreground extraction, one is with the initialization of bounding boxes i.e. by passing on the rectangular coordinates for the object that we want to segment (this process did not give good results and will be seen in detail in the Section 3.3.2.2) and other with the initialization of mask approximation i.e. passing a black and white mask similar to the shape of the object that needs to be segmented. The Grabcut algorithm then recursively applies the graph cuts to improve the segmentation from the approximate mask that is provided as the input [58]. In the mask initialization process the foreground is extracted using the resized image from Section 3.3.1 and the output image mask from Section 3.3.2.1.2 as input and passed onto the OpenCV function *'cv2.grabCut(image, mask)'*. Figure 3.8 below depicts the same.

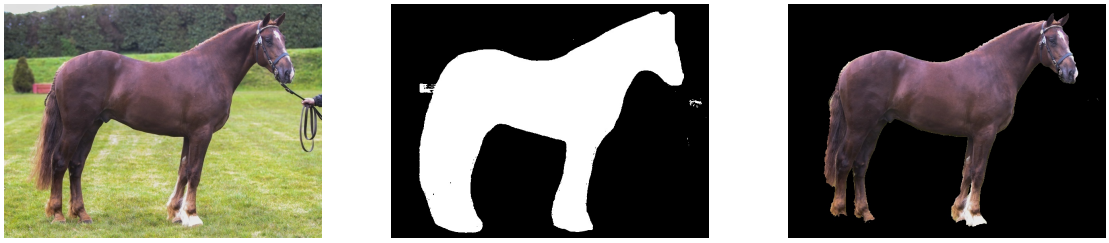

(a) (b) (c)

Figure 3.8: Foreground extraction of horse using mask approximation. **(a)** is the resized image from which the horse needs to be extracted. **(b)** is the approximate mask generated for the horse. **(c)** is the output image.

3.3.2.2 Approach that gave Poor Results?

3.3.2.2.1 Object Detection

The study uses the same model as used in Section 3.3.2.1.1 for object detection which is a bounding box around the object that is detected. This can be seen in Figure 3.4b. The coordinates for the rectangular box around the horse is *(50, 40, 750, 560)*.

3.3.2.2.2 Horse Extraction

This step takes in the resized image from Section 3.3.1 and rectangular coordinates of the horse detected in Section 3.3.2.2.1. These values are then passed onto OpenCV's Grabcut function *'cv2.grabCut(image, (50, 40, 750, 560)'*. Figure 3.9 below depicts the poor extraction results. This process yields poor results because coordinates need to be tuned/changed until the horse is properly extracted and requires manual intervention.

(a) (b) (c)

Figure 3.9: Foreground extraction of horse using bounding box approximation. **(a)** is the resized image from which the horse needs to be extracted. **(b)** provides the rectangular coordinates for the detected horse (50, 40, 750, 560). **(c)** is the poorly extracted output image.

3.3.3 Denoising

It is the process of removing high spatial frequency noise from an image. This is needed for better edge detection of the horse outline as it sharpens and smoothens the edges. This step takes in the output image from Figure 3.8c as input.

There are many algorithms available for denoising an image but the selection of these algorithms mostly depends on the type of noise an image contains. The image that the study processes mostly needs reduction of noise around the edges for proper edge detection. This type of noise is called salt-and-pepper noise. A study conducted by Pawan P. et al. [59] shows that Median filtering method is highly effective in removing salt-and-pepper noise.

Median filter takes in each image pixel and compares it with its neighbourhood pixel to decide whether the pixel is similar to its surrounding or not and if it is not similar then it replaces that pixel by the median values of the neighbourhood pixels [60]. An example of this can be seen in the below Figure 3.10.

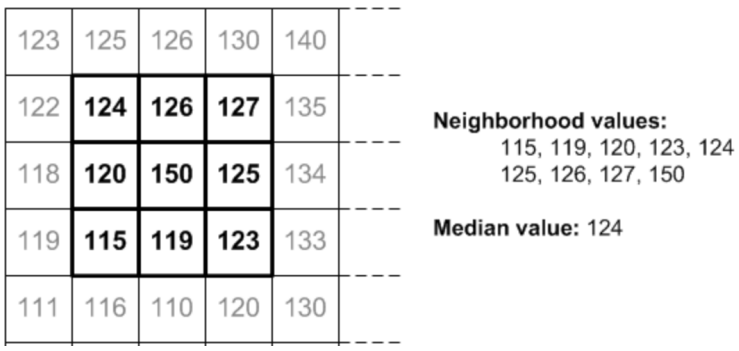

Figure 3.10: Median Filtering Technique. Image Source: [60]

From the image it can be seen that the central pixel value of 150 is not similar to its surroundings and so it is replaced by the median of its surrounding value 124. Larger the surrounding, better the noise reduction.

For the purpose of this research, OpenCV's Median Filtering [26] method is used for noise reduction *'cv2.medianBlur(image, kernel size)'*. The second parameter used is the *kernel size* which must be a positive odd integer and represents the size of the neighbourhood which needs to be considered. Kernel Size value 5 yielded the best results on visual comparison. The output of this process can be seen in Figure 3.11

(a) (b)

Figure 3.11: Denoising of the horse image. **(a)** is the foreground extracted horse image. **(b)** is the output received after applying median filtering.

3.3.4 Colour and Texture Analysis

Most of the research currently focuses on horse shape analysis using the outline landmark points around the horse. Colour and texture analysis is used for visual verification of angular proportions of the horse around the hip region because that is the most evident region where this analysis could be performed. When seen from the naked eye, the joints around the horse shows some darker shade and this existence of joints could be verified by using colour and texture analysis over the denoised horse image from Section 3.3.3.

The research uses Kmeans clustering algorithm for colour analysis of the image [48] [61] [49] [47]. Clustering is a technique of dividing data points into groups such that each group contains similar data points. These groups are known as clusters. In cluster based colour analysis the clusters are represented by colours. The reason for selecting Kmeans algorithm for colour analysis is because it works really good for small datasets. It looks at all the output generated at each iteration and so the output is slow but the results obtained is pretty good [62].

OpenCV's Kmeans clustering method [24] was used for the purpose of this research. It involves following steps:

- First of all the three-dimensional shape *(800, 588, 3)* of the image is converted into two-dimensional shape *(470400, 3)*. Here the number 3 represents the RGB channels of the image.

- In the next step the two-dimensional array is fit into the Kmeans algorithm *'labels, (centers) = cv2.kmeans(array, k'*. Here, *labels* consist of the label for each pixel i.e. which cluster does this pixel belong to, *centers* consists of the cluster centers and k represents the total number of clusters.

- In the final step, all the image pixels are converted to the cluster colour they belong to and finally the image is reshaped to original shape.

The algorithm performed best for *5* number of clusters based on the visual comparison among different cluster numbers *(3, 4, 5, 6)* as seen from Figure 3.12.

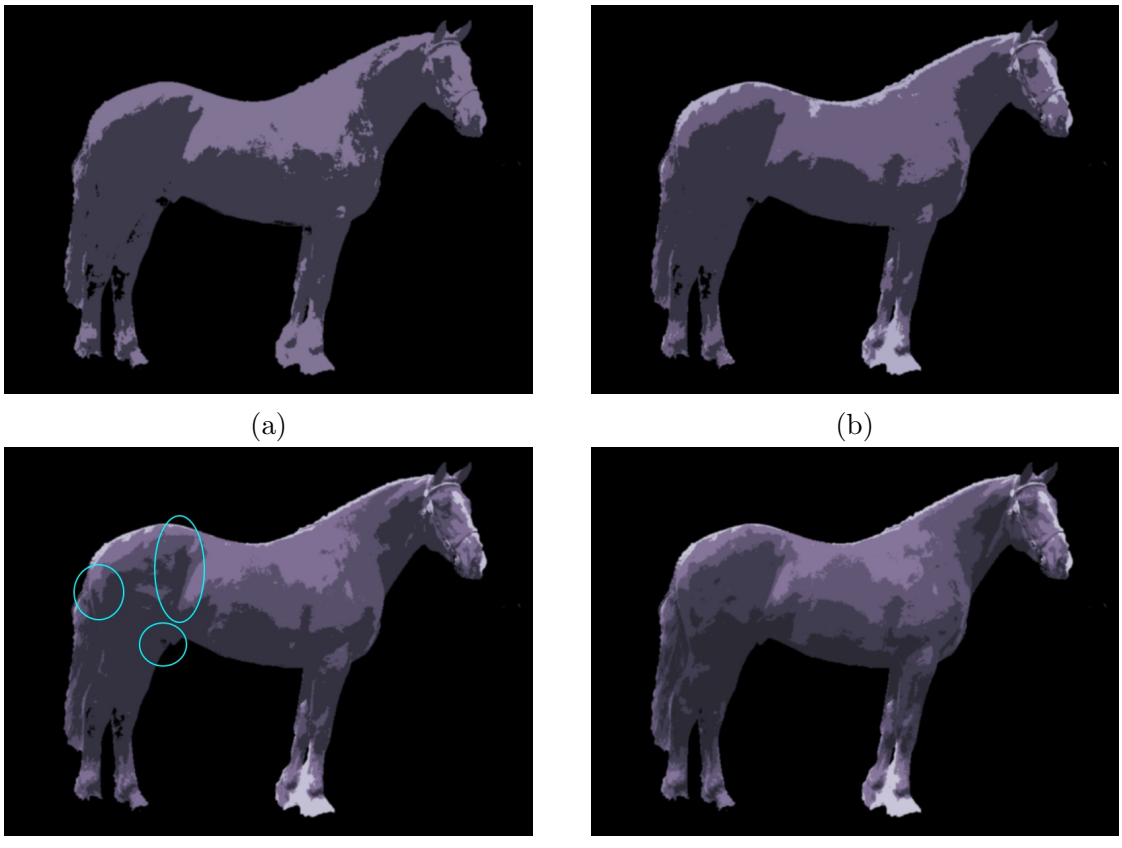

(a) (b)

(c) (d)

Figure 3.12: Colour Analysis over horse image for analysing visual verification for angular proportions using Kmeans clustering. **(a), (b), (c), (d)** are the output for (3, 4, 5, 6) clusters respectively. Cluster 5 gives best result and it can be seen in **(c)** that the circles (left, right, bottom) show the change of shade around buttock, hip and stifle joints region respectively.

The study uses the algorithm Local Binary Pattern (LBP) which is a textual descriptor made popular by the work of Ojala T. et al. [51] for texture analysis of the denoised horse image. The reason for selecting this algorithm is because it provides extremely fine grained details of the image [25] and has also been integrated with both OpenCV [12] and Scikit-Image [63] libraries.

LBPs compute a local representation of texture by comparing each pixel with its surrounding neighbourhood pixels. The LBP value for the center pixel is calculated and stored in an array of the same size as of input array.

The first step towards calculating a LBP value is to select a pixel and threshold the neighbouring pixels around it into binary form. Figure 3.13 show that for pixel value 4, all the neighbouring pixels that are greater than equal to center pixel are set to 0 and others are set to 1.

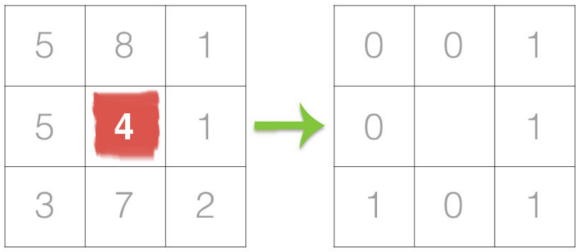

Figure 3.13: Calculating the LBP value of the center pixel 4. The first step is to threshold the neighbouring pixels in binary form. Image Source: [25]

The next step is to calculate the LBP value of the center pixel by selecting any neighbouring pixel and move in clockwise and anti-clockwise direction to create an array of string which is then converted into decimal form. Figure 3.14 illustrates the same. The above process is repeated until all the pixels in the array generate a LBP value for itself.

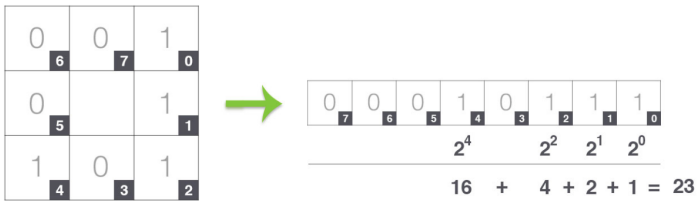

Figure 3.14: Converting the neighbouring pixels into decimal form to get the LBP value of the center pixel. Image Source: [25]

Scikit-image's implementation of LBP was preferred for the purpose of this research over OpenCV because OpenCV's LBP implementation works strictly for facial recognition and moreover, the scikit-image's implementation of the same provides grayscale invariance and rotation improvements for the image. For this implementation the denoised image from Section 3.3.3 is first converted into grayscale and the resulting array is passed onto the LBP function which in turn returns the new array with LBP values. Figure 3.15 below shows the result obtained. It can seen that circle numbered *1, 2, 3* shows the difference in shade, slight darker patch around the hip, buttock and stifle joints respectively. Similarly circle numbered *4, 5, 6* shows a slight dark patch around the hind leg knee joint, foreleg knee joint and elbow respectively.

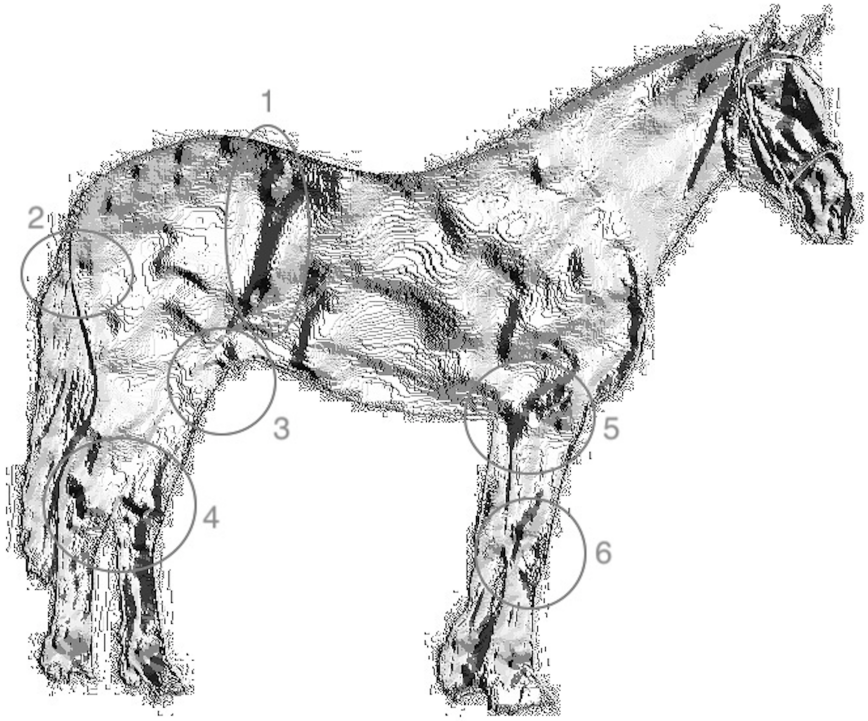

Figure 3.15: Texture Analysis over horse image for analysing visual verification for angular proportions using Local Binary Pattern.

Based on the colour and texture analysis results obtained above, it would be verified against the key points of the horse detected in later Section 3.3.7. It would be seen if the location of dark patches that denote bone joints and the key joints detected via the algorithm match with each other or not.

3.3.5 Contour Detection

It is the process of detecting the outline and edges of the horse. These outline will further be used to detect the corners and points of interest. This step takes in the denoised horse image from Section 3.3.3 as input. Contour/Edge Detection requires denoised image instead of original image because denoising of images sharpens and smoothens the edge of the image along with removing the extra noise which might result in wrong edge detection.

3.3.5.1 Approach that gave Good Results?

This study uses the Holistically-Nested Edge Detection (HED) architecture proposed by Saining X. et al. [46]. It is a deep neural network based architecture which takes in a RGB image as input and produces the edge map of that image as an output. The reason for selecting HED for the scope of this study was because it is the most popular deep learning framework with maximum accuracy and speed available as compared to other deep learning based architectures like [42] [43] [44] [45]. The HED model has also been included in the OpenCV's DNN module for edge detection which requires OpenCV version 3.4.3 or higher [64]. HED architecture uses convolutional neural network for prediction of edges and the output generated by each layer is used as a side output by next layer and finally all these outputs are fused together to generate final edge map. The architecture of HED model can be seen in [46] [64].

For the purpose of this study, a pre-trained HED model is used for edge detection [23]. This model has been trained on NYU Depth Dataset [65] and Berkley Dataset [66]. The reason for selecting this model was because it gave state-of-the-art results on both these datasets. Figure 3.16b below shows the result for HED model. It is evident from the output that the edge detection gave good results even in difficult areas like the ear and hind legs.

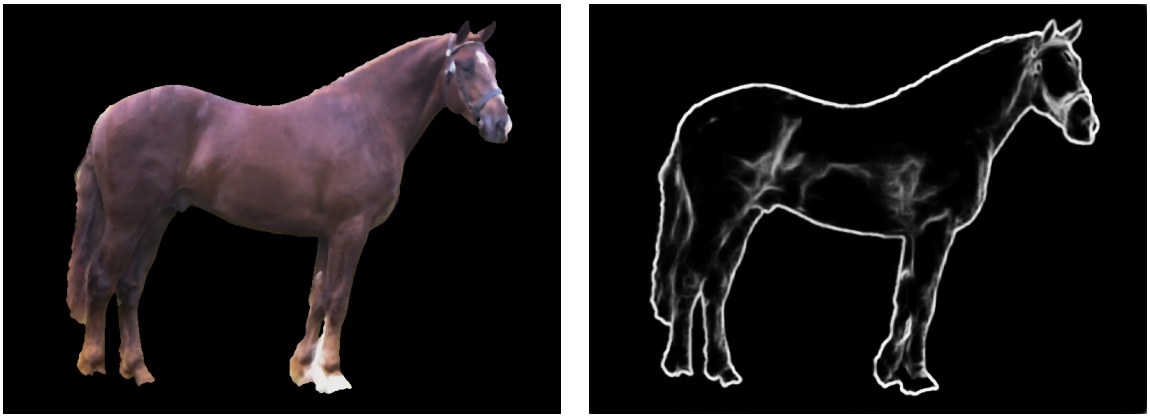

(a) (b)

Figure 3.16: Edge Detection using Holistically-Nested Edge Detection CNN model. **(a)** is the denoised horse image. **(b)** is the output image obtained.

3.3.5.2 Approach that gave Poor Results?

Another approach that was tried for edge detection of the horse image is the use of OpenCV's Canny Edge Detector (CED) [14] method which has been the go-to-method for edge detection before the development of deep learning based models. CED detects edges based on the change in intensity. CED uses three parameters for edge detection *'cv2.Canny(image, minThresholdValue, maxThresholdValue)'*, where *minThresholdValue* is the lower threshold value selected in a way that any pixel having gradient value below this value is not an edge and *maxThresholdValue* is the higher threshold value selected in a way that any pixel having gradient value higher than this value is an edge. Figure 3.17b below shows the output of Canny Edge Detection. The reason why CED did not give good results are:

- CED focuses only on the local changes i.e. it lack semantic understanding of the content in the image.
- The setting of lower and upper threshold values is a manual process and needs to be changed for different image.
- The thresholding works differently for different image with varying lighting conditions.

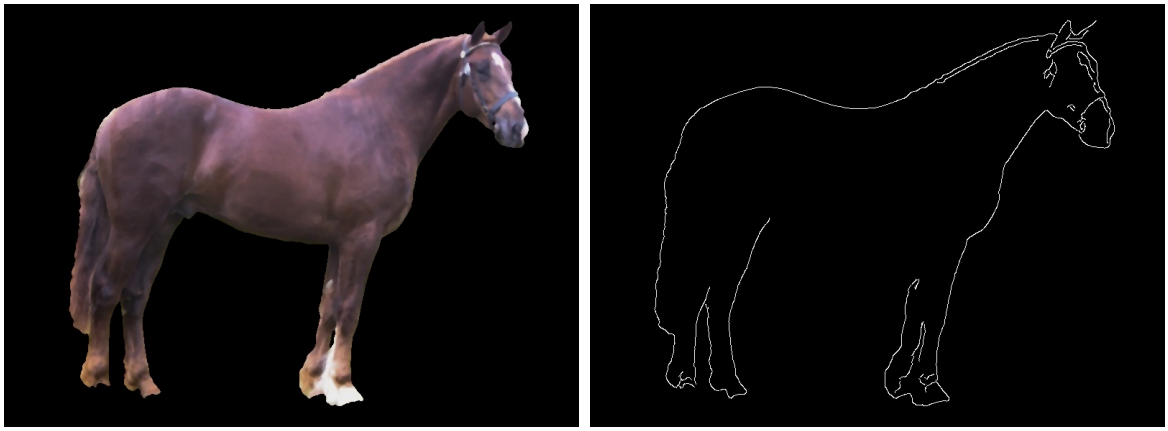

(a) (b)

Figure 3.17: Edge Detection performed using Canny Edge Detector Algorithm. **(a)** is the denoised horse image. **(b)** is the poorly edge detected output image obtained.

3.3.6 Corner Detection

Feature detection and matching is the most important part of a Computer Vision application, which requires finding the correspondence between features within images. A corner, which is a special point in an image, is a type of feature. The local feature of a corner is called a "key feature point" or "point of interest" or "corner point" [67]. This step takes in the edge detected image generated in Figure 3.16b as input for corner detection. These corners then detected are used to select key points of interest for horse conformation analysis.

There are many corner detector algorithms available with the most common one being OpenCV's Harris Corner [15] method and Shi-Tomasi [27] method. This study used Shi-Tomasi Corner Detector method proposed by Shi et al. [68] for detecting corners around the edge detected image. The Shi-Tomasi algorithm is an improvement of the Harris algorithm and the difference just lies in the way the value of R score is calculated for comparison of corner intensity.

The Harris corner method has a selection criteria for determining corners. It first calculates the score of pixel using two eigenvalues which are passed to a mathematical function to get the score. If this score is above a threshold value then it is marked as a corner. However, Shi-Tomasi just made a minor change in the way the score was

calculated by directly using the eigenvalues to determine if the pixel was a corner or not. It has been demonstrated by the study in [69] [70], that Shi-Tomasi performs better in corner detection than Harris Corner. This was the reason for selecting Shi-Tomasi over Harris Corner detection.

Another advantage of selecting Shi-Tomasi over Harris is that it also provides the ability to select only the top corners through a parameter value. Harris corner algorithm also requires the change in the threshold value until the corners are detected properly which needs to be changed for every image.

For the purpose of this study, OpenCV's Shi-Tomasi method was used with following parameters, *'cv2.goodFeaturesToTrack(image, maxCorners=200, qualityLevel=0.02, minDistance=20)'*, where *maxCorners* defines the total number of corners selected, *qualityLevel* defines the minimum quality of corners that need to be selected and *minDistance* defines the the minimum distance between these corners in pixels. Figure 3.18 shows the output obtained for both the algorithms.

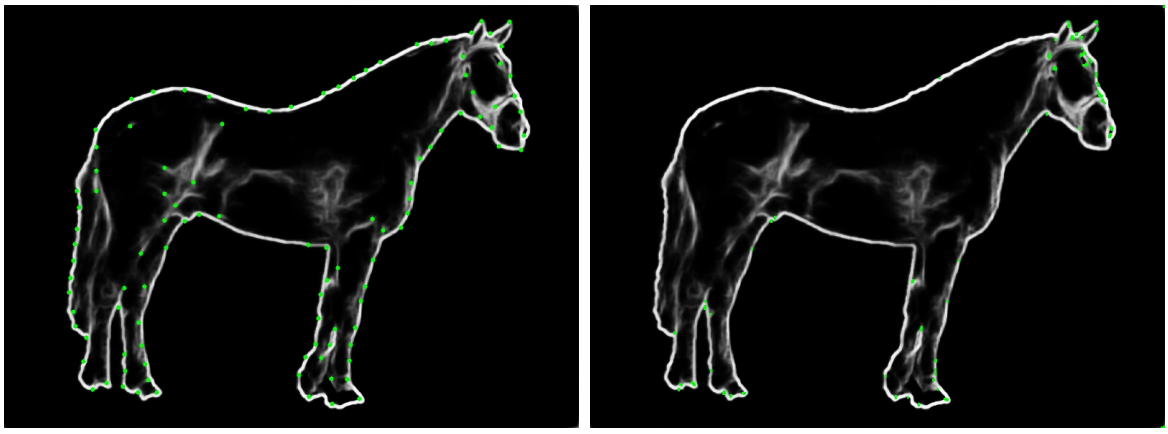

(a) (b)

Figure 3.18: Corner Detection performed on the Edge detected image. The green dots in the image represents the corners detected. **(a)** is the result obtained after applying Shi-Tomasi Algorithm. **(b)** is the result obtained after applying Harris Corner Detection Algorithm.

It is evident from the above Figure 3.18 that Shi-Tomasi algorithm performed better in corner detection (Figure 3.18a) than Harris Corner (Figure 3.18b). Harris corner detector missed most of the corners around the hind leg region, hip region and underline region of the horse.

3.3.7 Novel Algorithm to Detect Key Points of Interest

This step detects all the key points of interest from the corners detected via Shi-Tomasi algorithm (as seen in Figure 3.18a). The study proposes a novel algorithm for the purpose of key points detection using the extreme left, right, top and bottom points around the edge of the horse along with finding out the center of gravity of the horse. These key points detected would be used for horse conformation evaluation and scoring. The detection of key points proceeds in two steps:

3.3.7.1 Extreme Points Detection

The first step is to detect the extreme left, right, top and bottom points around the edge of the horse image along with finding out the center of gravity of the horse. Figure 3.19 below depicts the same. The yellow circles around the edge of the horse shows extreme points detected. The yellow circle in the center of the horse shows the center of gravity. These extreme points are calculated using the *argmin & argmax* function provided by Python which takes array of coordinates as input [20] and the center of gravity is calculated using the *OpenCV's Moments* function which takes the horse contour as input [71].

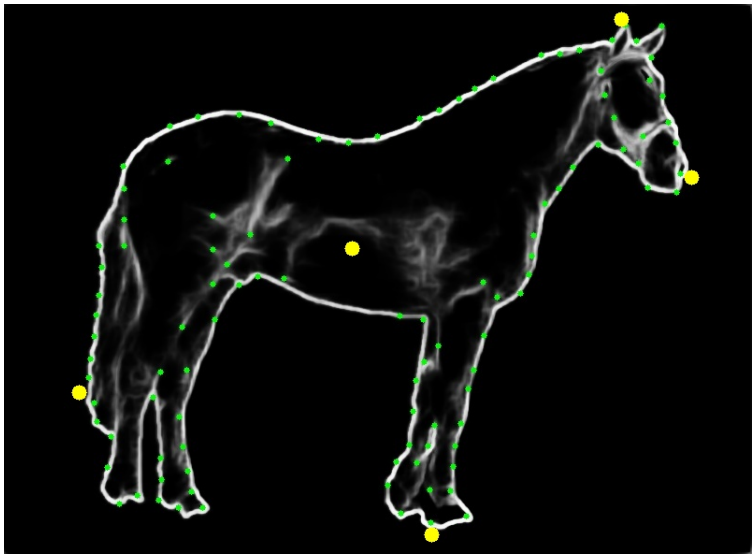

Figure 3.19: The yellow circle around the edge denotes the extreme left, right, top and bottom points. The yellow circle in the center of the horse denotes the center of gravity of the horse.

3.3.7.2 Image Flipping

For the purpose of identifying the key points, the algorithm needs all the horses to be aligned/standing in the same direction i.e. the head of the horse should be on the right side of the image. This step takes the extreme points detected in Figure 3.19 as input. The extreme top point helps in identifying the alignment of the horse. If the x-coordinate of the extreme top point is greater than the half of the width of the image then the horse is standing with its head on the right and if the extreme top point is less than the half of the width of the image then the horse is standing with its head on the left of the image. In this scenario the image is flipped, along with all the previous images of the horse obtained in earlier steps. Figure 3.20 depicts. In the below Figure 3.20a, the x-coordinate of the extreme top point of the horse is 100 which is less than the half of the width of the image 400. Therefore the image is flipped as seen in Figure 3.20b.

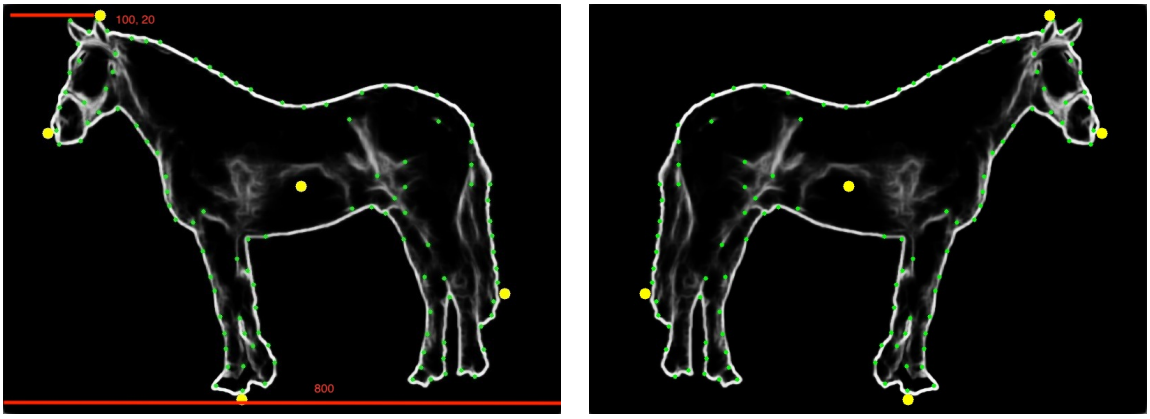

(a) (b)

Figure 3.20: Image flipping performed to align all the horses to be standing with its head on the right of the image. **(a)** The x-coordinate for the extreme top point in the image is less than half of the width of the image. **(b)** Flipped image.

3.3.7.3 Key Points of Interest Detection

This is final step towards detecting the key points of interest from the corners, extreme points and center of gravity of the horse obtained. Since, the horse image is first of all resized to a scale factor set to width 800, therefore, for the detection of key points

a certain range in pixel is used from these points. This new coordinate looks for the closest corner in around this point by calculating the distance between the each of the corners available. Figure 3.21 below shows the flow of key points detection using these yellow circled points.

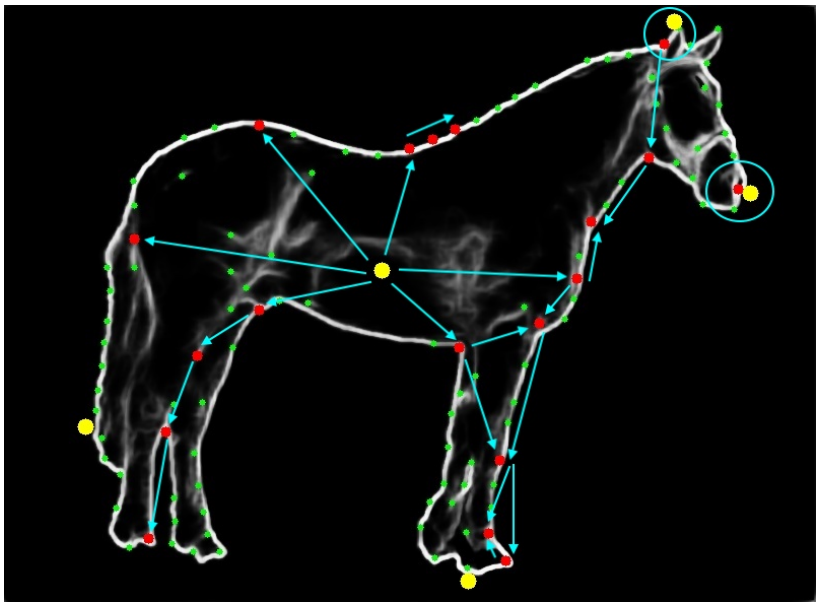

Figure 3.21: Detection of key points of interest using the extreme left, right, top, bottom and center of gravity points. The red dots in the image are the key points of interest detected. The blue arrow shows the flow of point detection along the influence of coordinates on selection of a particular point.

From the Figure 3.21 above it can be seen that each yellow circle point derives the selection of a particular point which in turn influences the selection of other points.

- The center of gravity derives the algorithm to locate these point directly *(Hip, Wither, Stifle, Point of Shoulder, Elbow and Point of Buttock).*
- The extreme right points helps in detection of *Muzzle.*
- The extreme top point helps in detection of *Poll* which in turn influences the detection of *Throatlatch, Neck Joint.*
- The extreme bottom point helps in locating the coordinate for the bottom part of the horse which in turn help in calculating the height of the horse from *Wither to Ground and from Hip to Ground.*

Chapter 4

Horse Conformation Evaluation

In order to achieve the research objective, the final step is to analyse the Good Balancing traits of a horse. Balance is arguably the most important criteria for evaluating the calibre of a horse in terms of both quality and performance. It refers to proper blending of all the horse's body parts and muscling. The muscling must have proper evenness and must present a pleasing picture of the horse. Proper balance gives the horse more power and smoother movement [3]. The internal body capacity of a horse indicates the space available for the proper functioning of heart and lungs i.e. with more lung capacity, the horse can take in more air after each step making it the movement powerful [9].

The traits which are going to analysed are mentioned in Table 1.1 for measuring angular proportion and Table 1.2 for measuring body length proportion. The body length is calculated in pixels.

4.1 Body Length Proportion

For evaluating the body length proportion the distance between two points was calculated the using formula [72],

$$\sqrt{(X_2 - X_1)^2 + (Y_2 - Y_1)^2}$$

where $(X_1, Y_1)\&(X_2, Y_2)$ are two coordinates.

4.1.1 Trait: Body Shape

The most important aspect when determining the balance of the horse is whether the horse is carrying equal weight on its front end and back end. The horses skeletal structure helps in determining the correct proportion of horse's body parts. The *length of Neck, Shoulder, Back and Hip should be approximately equal* [3] [7]. Figure 4.1 shows the length of different parts obtained which are approximately equal to each other.

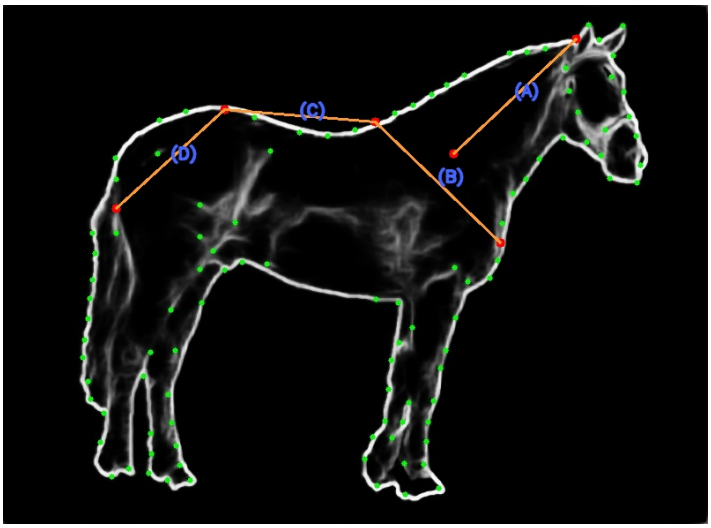

Figure 4.1: **Length from (A) to (D): (190, 197, 172, 166)**. An example illustration of *(Trait: Body Shape)* shows that the length of different body parts calculated are approximately equal to each other A = B = C = D. This depicts that the horse carries equal weight from front to the back.

4.1.2 Trait: Body Direction

This is one of the most important criteria to be considered while evaluating the balance of a horse. The topline (measured from wither to the point of hip) must be shorter than the underline (measured from point under the belly to stifle). A longer topline indicates that the horse has a long and weak back which makes the movement of the horse difficult [3] [7]. It also makes it difficult for the horse to bring its hind legs under the body which is the source of power for a horse to move forward. From the Figure 4.2 below it can seen that the horse has a shorter topline than underline.

Another important criteria considered here is that the *height of the hip must be equal to the height of the wither*. If the wither is lower than hip height, then the horse is a *downhill* horse which means that the horse would carry a lot of weight on its forehand and would lack driving power and maneuverability. Also, if the horse carries to much weight on its forehand, then it would lead to lameness. However, if the wither height is higher than hip height then the horse is a *uphill* horse and often uphill horses are not penalised during conformation evaluation [3]. From the Figure 4.2 below it can been seen that the horse is a downhill horse. The pink line in the image denotes the same.

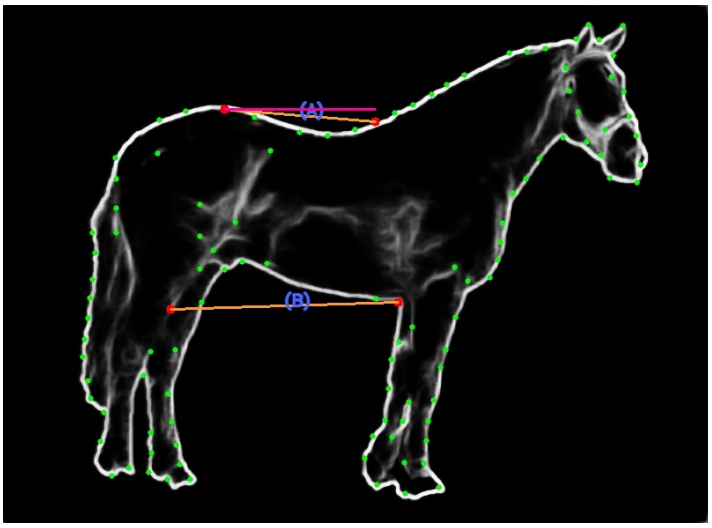

Figure 4.2: **Length from (A) to (B): (172, 258)**. An example illustration of *(Trait: Body Direction)* shows that the topline (A) is shorter than the underline (B) and the pink line denotes that the horse is a downhill horse. This depicts that the although the horse has ideal topline to underline ratio but it carries more weight of forehand because it is a downhill horse.

4.1.3 Trait: Body Capacity

The body capacity of the horse determines whether a horse has enough room for the proper functioning of heart and lungs. With larger lung capacity, the horse can take in more air with every step, making it more powerful with the increase in stamina. The body capacity also determines the possibility of large broodmare to convey a large foal

[9]. From the Figure 4.3 below three conditions needs to be satisfied to measure the body capacity of a horse:

- The depth of heart girth (measured from wither to chest floor) (Length A) must be equal to length from chest floor to fetlock point (Length B).
- The depth of heart girth (measured from wither to chest floor) (Length A) must be greater than depth of flank (measured from hip to stifle) (Length D)
- The length of depth of heart girth (Length A) + length from chest floor to fetlock point (Length B) + length from fetlock point to ground (Length C) should be equal to length from point of buttock to point of shoulder (Length E).

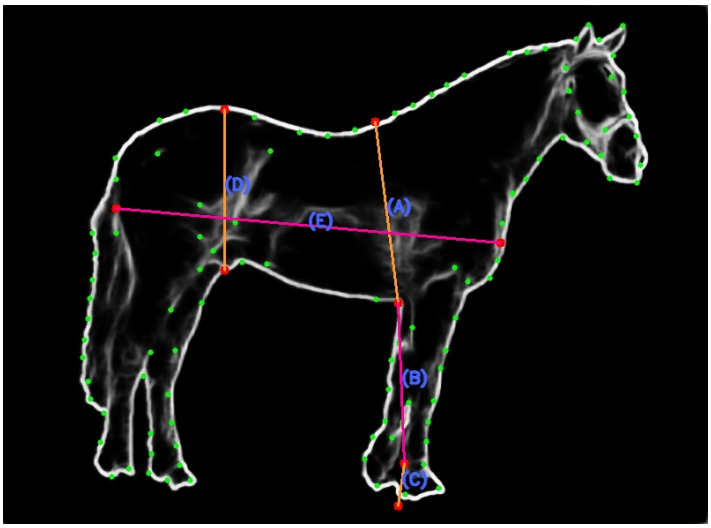

Figure 4.3: **Length from (A) to (E): (207, 182, 49, 182, 438)**. An example illustration of *(Trait: Body Capacity)* shows that the depth of heart girth (A) is approx. equal to the length from chest floor to fetlock (B), the depth of heart girth (A) is greater than the depth of flank (D) and the height from wither to ground (A+B+C) is equal to length from buttock to shoulder (E). All these ideal conditions depict that the horse has good depth of heart for proper functioning of the vital organs.

4.1.4 Trait: Ratio of Length of Top and Bottom Neck

Another very important ratio that needs to be considered while evaluating the conformation of a horse is the ratio of the topline of the neck to the underline of the neck.

The topline of the neck is measured from poll to the wither whereas the underline is measured from throatlatch to the point of shoulder. The ideal ratio of the topline to the underline should be 2:1.

The ideal ratio of the neck allows the horse to have a proper sloped shoulder because the wither is well behind the point of shoulder. This gives the horse the ability to flex at the poll keeping the neck in slight arch. A horse that has longer underline will have straight shoulders reducing the ability of the horse to flex and lower its head. This type of a horse is called 'ewe necked' horse [3]. Figure 4.4 below shows the ratio of topline to the underline obtained. The ratio obtained shows that the horse has an ideal topline to underline ratio having a proper sloped shoulder.

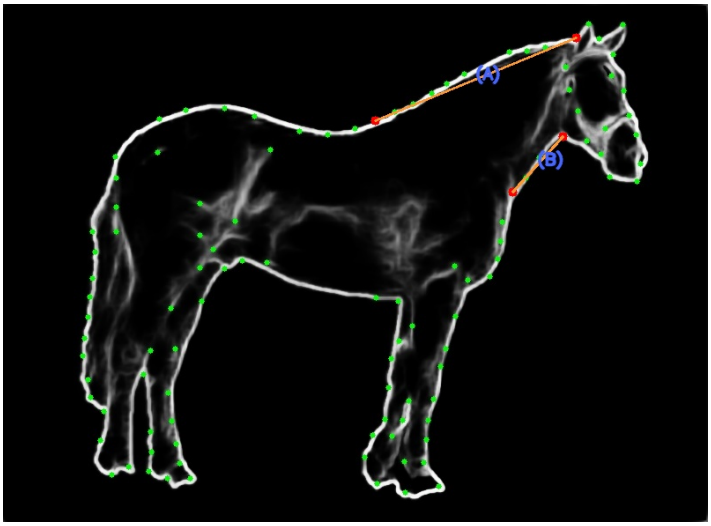

Figure 4.4: **Length from (A) to (B): (217, 98)**. An example illustration of *(Trait: Ratio of Length of Top and Bottom Neck)* shows that the length of topline (A) (measured from poll to wither) is approx. twice the length of the underline (B) (measured from throatlatch to point of shoulder). This depicts that the horse has an ideal range of topline to underline ratio thus, giving the horse an ability to flex at the poll.

4.1.5 Trait: Distance from Poll to Throatlatch and Poll to Muzzle

The ratio of the length measured from poll to throatlatch (windpipe) with respect to the length measured from Poll to Muzzle is another important trait to be considered

for evaluating the conformation of a horse. The length from poll to throatlatch should be roughly half the length from poll to muzzle [3].

If the distance from poll to throatlatch is longer than the ideal length, then the ability of the horse to flex around the poll decreases. It also creates a breathing problem in the horses, when the horse moves its head towards the chest. Figure 4.5 below shows the ration of the length of throatlatch to the head. The ratio obtained shows that the horse has an ideal length of the throatlatch with respect to the head.

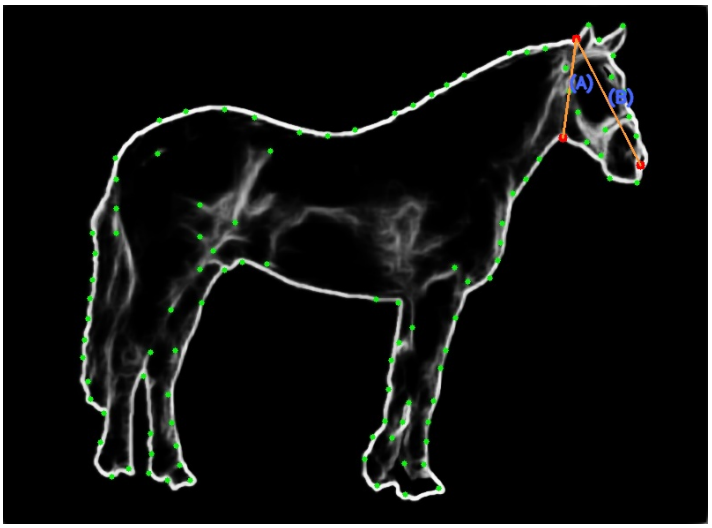

Figure 4.5: **Length from (A) to (B): (103, 181)**. An example illustration of *(Trait: Distance from Poll to Throatlatch and Poll to Muzzle)* shows that the length from Poll to Throatlatch (A) is approx. half the length from poll to the muzzle (B). This depicts that the horse has an ideal ratio of length of throatlatch to the length of head thus, the horse would have proper breathing patter.

4.1.6 Trait: Length of Neck

One of the most important factors to be considered while evaluating the horse conformation is the length of the neck of the horse. The length of the neck contributes to greater agility, freer movement and balance of the horse. It also helps in maintaining the balance of the horse while the horse swings its head and neck, up and down and also stretches forward and backward. Excessive long neck reduces the agility and balance of the horse because the center of gravity of the horse moves too forward. With longer

neck the distance between the joints increases thus reducing the ability of the horse to flex [4].

As seen from the Figure 4.6 below, in order to measure the ideal length of the following conditions must be satisfied:

- The length of neck (B) (measured from poll to wither) must be approximately one and half times of the length from poll to muzzle (A).
- The length of neck (B) must be approximately one-third of the total length of the horse (C).
- The length of neck (B) must be approximately equal to the length from elbow to hoof (D).

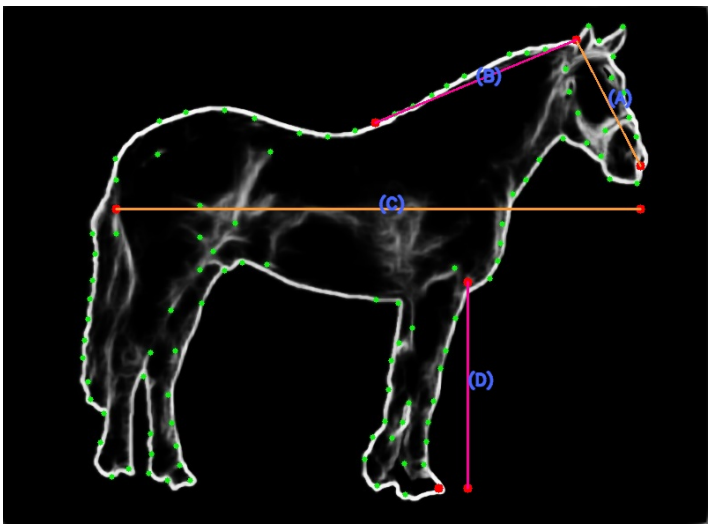

Figure 4.6: **Length from (A) to (D): (181, 227, 595, 234)**. An example illustration of *(Trait: Length of Neck)* shows that the length from Neck (B) (measured from poll to wither) is approximately 1.5 times of length from poll to muzzle, approximately 1/3 times of length of the horse and approximately equal in length from elbow to hoof. This depicts that the horse has an ideal neck length thus giving the horse greater agility and balance.

4.1.7 Trait: Wither and Hip Height from Ground

This trait is similar to the trait Body Direction where the wither height was measured to determine if the horse is a downhill or uphill horse [6]. The length of wither from ground and the length of hip from ground must be equal is length. This determines whether the horse has proper balance. The point on the ground is detected using the extreme bottom point detected in earlier section. Figure 4.7 below illustrates the same.

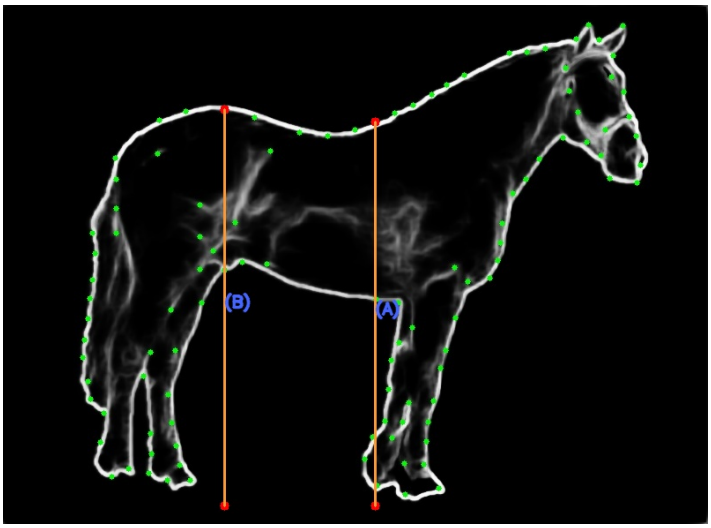

Figure 4.7: **Length from (A) to (B): (435, 449)**. An example illustration of *(Trait: Wither and Hip Height from Ground)* shows that the wither height (A) is approximately equal to the hip height from ground (B). This depicts that the horse has proper balance.

4.2 Angular Proportions

For evaluating the angular proportion the angle between three points was calculated using thw formula mentioned in the study [73]. The intersection of three points was used to calculate the angle of the intersection point. In Table 1.1, the *center* column represents the intersection point.

For the purpose of this study multiple joint angles were evaluated which influences the balance the horse. The most important joint angle calculated was the shoulder slope angle [3]. The shoulder slope is calculated by drawing a perpendicular line from

the scapula to the ground and another line is drawn from the wither to the point of shoulder. The intersection of the same should have an ideal angle of 45°. The shoulder slope of a horse influences the stride length and smoothness and a straighter shoulder could make it difficult for a horse to extend its front legs. Figure 4.8 below depicts the shoulder slope calculated.

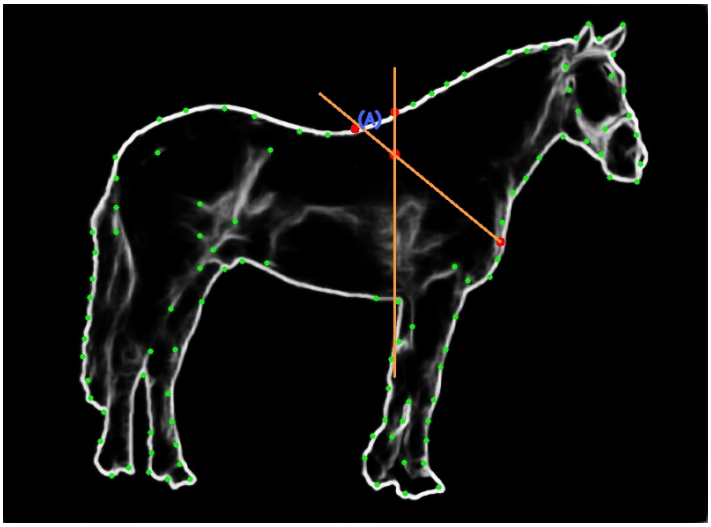

Figure 4.8: **Angle (A): (50°)**. An example illustration of the *(Shoulder slope)* shows that the horse has an approximately ideal angle thus having longer stride and smoothness in its movement.

Joint angles around the shoulder and hip region govern how smooth a horse will be in its movement. A good sloped shoulder acts as shock absorber. The sharper the angle around the shoulder and hip region, the greater the range of motion in legs. Following angular proportion are considered for a good sloped shoulder along with hip region [4]. As seen in Figure 4.9 below, following angular proportions must be satisfies for a good sloped shoulder and hip region:

- Should have an ideal angle of 60° from the line of point of shoulder to the junction of neck and wither (A).
- Should have an ideal angle of 40°from the line of point of shoulder to the junction of neck and back (B).
- The angle made by horizontal line drawn from point of shoulder and the line drawn from point of shoulder to wither (C) must have an ideal angle of 50°.

- The angle formed by the line drawn from hip to stifle, stifle to point of buttock and point of buttock to hip must form an equilateral triangle (D, E, F) i.e. it must ideally have an angle of 60° each.

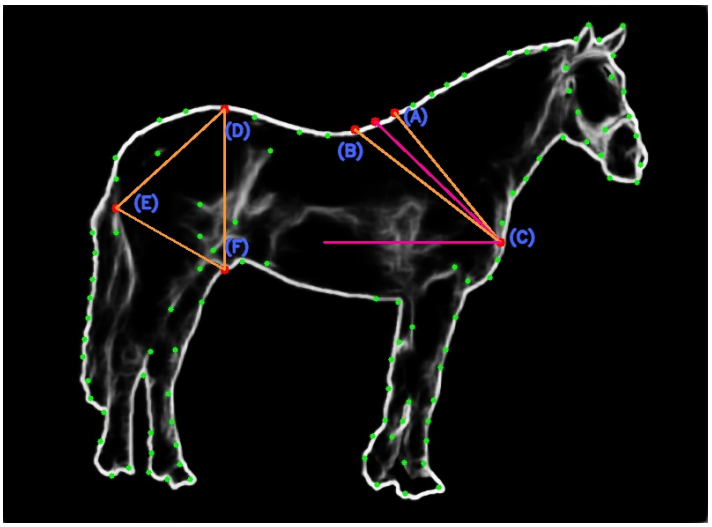

Figure 4.9: **Angle (A) to (F): (68°, 59°, 45°, 48°, 72°, 60°)**. An example illustration of the *(Shoulder slope and hip region angles)* shows that the horse would have difficulty in motion due to greater shoulder and back junction slope (B) and point of buttock angle (E).

A study presented by [5] shows the range of angles obtained for particular joints in order to determine the good balance of the horse. To improve the conformation traits, a range of angles was calculated by using 243 Franches-Montagnes stallions. The repeatability and consistency of the extracted joint angles assessed to define an ideal range which would further help in analysing the conformation of other horses.

Figure 4.10 below shows the calculation of some of the joint angles. The joint angles around the fore and hind legs was not calculated because of the difficulty in extracting the shape of the hoof region of the horse (horse standing in a grassy area). Table 4.1 below shows the range of angle for a particular joint and obtained result.

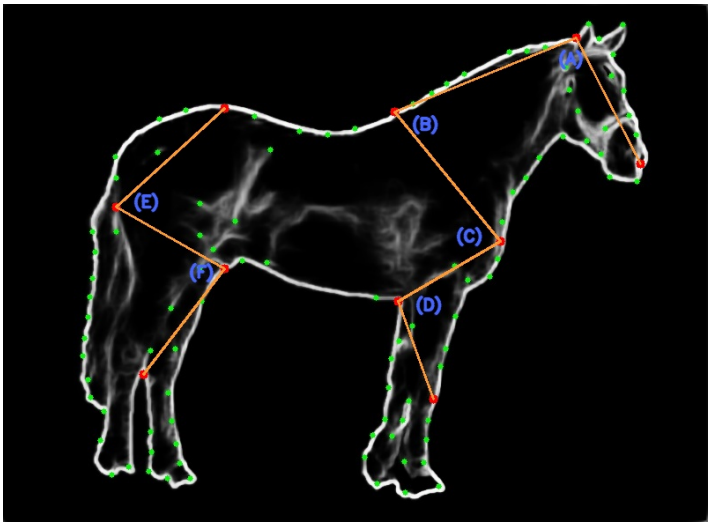

Figure 4.10: **Angle (A) to (F): (95°, 73°, 81°, 101°, 72°, 82°)**. An example illustration of the *(structural angles)* shows that the horse would have difficulty in motion due to greater shoulder and back junction slope (B) and point of buttock angle (E).

Angle Name	**Min**	**Max**	**Angle Calculated**
Poll joint (A)	92°	117°	95°
Wither joint (B)	64°	99°	73°
Shoulder-Elbow Joint (C)	77°	122°	81°
Elbow joint (D)	109°	146°	101°
Buttock joint (E)	70°	88°	72°
Stifle-Hock joint (F)	87°	122°	82°

Table 4.1: The result obtained after calculating the structural angles. The source of the range of angles (Min and Max) is [5]. The table depicts that most of the structural angles of the horse lies in the ideal range thus giving a confidence for the ideal balance of the horse.

Chapter 5

Results and Discussion

For the purpose of determining the calibre of the horse, the overall conformation score of a horse needs to be calculated. The angular proportions around the hip region will also be visually verified by plotting the key points of interest over the colour and texture analysis images generated. Apart from the conformation scoring and angular proportion analysis, this section also presents the system verification, which was performed on 30 horse images to determine how well did the algorithm work in analysis of horse conformation. Finally the limitations of the system will highlight the potential problems in the system along with suggesting some probable solutions for the same.

5.1 Evaluation

5.1.1 Conformation Scoring

The measurement the conformation traits calculated in Section 4.1 and Section 4.2 are used for evaluating whether the horse is Good Balanced or not. The horse is evaluated by giving a +1 score for every conformation trait it has and based on how high the score was achieved, the horse's quality is given. The total number of traits for Body Length Ratio (11) are defined in Table 1.2 and for Angular Proportions (12) are defined in Table 1.1.

Since the calculation of exact length and angle is tricky, therefore the algorithm has been trained to consider a range of $\pm$ 30 pixels for body length ratio and a range of $\pm$ 5° for angular proportions. On evaluation, the horse is rated based one of the three

qualities: Poor, Average and Good Balanced. Out of a total of 23 traits, if the score obtained is less than 15/23, then the horse is Poor Balanced, if the score obtained is in between 15/23 and 18/23, then the horse is Average Balanced and if the the score obtained is greater than 18/23, then the horse is Good Balanced.

The horse image used in all the section in the thesis has been taken from Stallion Selection for Horse Sport Ireland 2019 [28] and it scored 10/11 in Body Length Ratio and 9/12 in angular proportion. The total score obtained is 19/23 which shows that it is a Good Balanced horse.

The above rating and score of horse conformation traits is based on learning's from the Conformation Document [1] [3] [4] [6] [7] [8] [9] [10]. The Actual plan was to get this verified by actual Horse Breeder and test it on some images captured personally or collected through him, but could not get his verified due to Covid-19 conditions.

5.1.2 Visual Verification of Hip region points using Colour and Texture Analysis

The joint angles obtained around the hip region (hip joint, stifle joint and buttock joint) will be visually verified by merging the key points of interest over the Colour analysis image (Figure 3.12c) and Texture analysis image (Figure 3.15). This visual verification provides confidence about the existence of joints in correct place as identified by the change in shade of those region.

From the visual verification of texture analysis image (Figure 5.1a), it can be seen that the hip joint, buttock joint and stifle joint are located around the black patch inside the circle number 1, 2, and 3 respectively, thus, depicting that the joint angles formed around these points are located correctly. Apart from this, the texture analysis also indicates the knee point detected in circle numbered 4 and 6. The black patch in circle numbered 5 also show the elbow point detected around that region. The dark patches in the image shows the movement and presence of some sort of bone structure around that area.

From the visual verification of colour analysis image (Figure 5.1b), it can be seen that in this case also the change of shade to dark purple around the right, left, and bottom circle shows the presence of hip, buttock and stifle points respectively. However, the colour analysis technique does not show the presence of any other joint angles in

the image. Thus, when compared, texture analysis over horse image appears to be a better visual indicator of the bone structure of the horse.

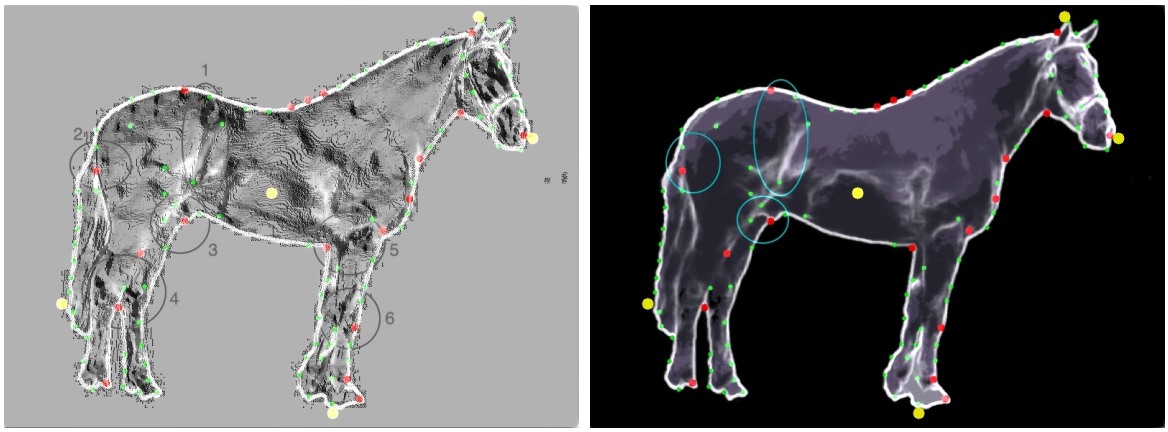

(a) (b)

Figure 5.1: Visual Verification of Hip region points using Colour and Texture Analysis. **(a) & (b)** is the texture analysis image and it clearly shows the presence of hip, buttock and stifle joints in the circle number 1, 2, 3 respectively. However, texture analysis over horse image appears to be a better visual indicator of the bone structure of the horse.

5.2 System Verification

In order to verify that the algorithm detects the key points in a correct way to calculate the proportions of the horse, it was tested on a total of 30 horse images collected from Google Images (5) and *Stallion Selection for Horse Sport Ireland 2019 and earlier (25)* [28]. The reason for selecting testing samples from two different places was because the horse's from Horse Sport Ireland was mostly used for sporting events, thus depicting that they might have good conformation. So to get a variation in the results the horse image from two different place were selected.

Another selection criteria for the horse image was the colour of the horses for verifying the results of foreground extraction and colour and texture analysis. *Horses of colour white (6), black (6), brown (6), mixture of black and brown (6) and white textured (6) were selected.*

The things that were noted while detecting the horse conformation over a sample of 30 horse images are:

- Around 20/25 horses from Horse Sport Ireland score good conformation score and were rated as Good Balanced, while the horse images (5/5) obtained from Google Image scored average conformation score and were rated as Average Balanced.
- The detection of key points of interest is independent of the colour of the horse. This can seen from a sample of good conformation results obtained in Figure B.1.
  - Most of the horses scored higher point in Body Length Ratio Proportion.
  - For Angular proportion most of the horses showed deviation from the ideal range around the hip angle and wither angle region.
- Around 8/30 horses showed deviation in detection of the key points of interest, although each one of them scored good conformation results and were rated as Good Balanced by the algorithm. The measure of error displacement in key point location can seen from Figure B.2.
  - The region where most issues were noted are Hind leg, Hoof region and Buttock. This may be due to the different hind leg standing position of the horse.
  - The displacement of key points noted was just the next point which was due to algorithm looking for closest node around that particular node.
  - The maximum number of displacements noted in an image was 6 out of the 20 corner points detected by the algorithm.
  - However, since the displacement was very minor (around 20 pixels), therefore it did not affect much in the Evaluation of Body Length Proportion, but it showed a slight deviation in the evaluation of angular proportions.
- Colour analysis on horse image for visual verification of angular proportions around the hip shows that the it did not give proper results for white coloured horse image. This maybe due to the insignificant change in colour shade around the joint angle of the horse. However, it worked properly when texture analysis

algorithm was applied to the same horse. This is one of the limitations of the algorithm and will be discussed in detail under the Limitations section 5.3.

The result obtained by running the algorithm over a sample of 30 images gives a positive confidence in the the output obtained which is very close in some cases if not accurate. The results show that the algorithm worked as it was intended to work, but shows some deviation in the detection of key points. Overall, the algorithm worked well to assess the horse image in providing the quality of the horse, but it can surely be improved and the same would be discussed in detail in the Future Work section 6.2.

5.3 Limitation

5.3.1 Stance and Shape of the Horse

The basic requirement of an horse image dataset is that all horse images must be similar to each other in terms of standing position and shape of the horse. The hind and fore legs must be clearly separated, the head of the horse must not face the camera but to the side. This greatly influences the detection of key points around the hind leg region (knee, hoof) and neck region (throatlatch).

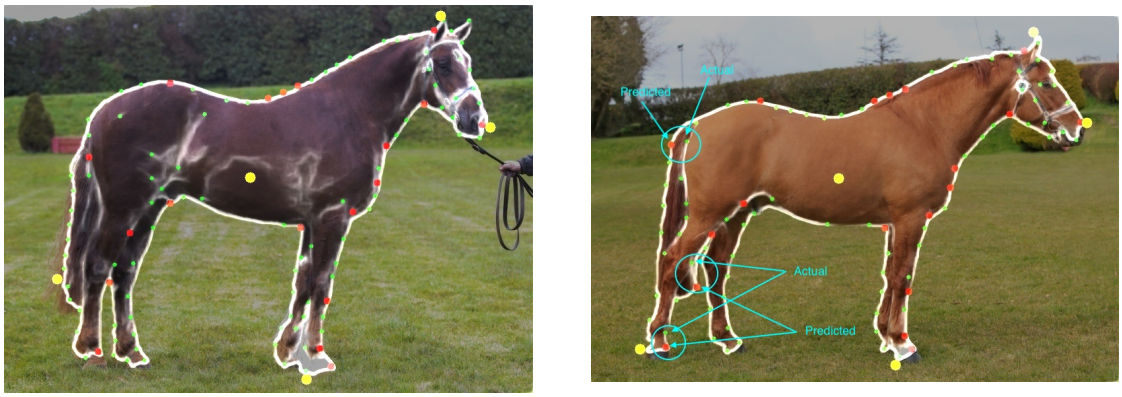

(a) (b)

Figure 5.2: **(a)** Ideal key points detected of the horse. **(b)** it can be seen that the gap between the hind legs leads to deviation in the detection of points in that region. Another reason is the length of the horse which leads to wrong detection of buttock point.

From the Figure 5.2 above, it can seen how the stance of hind legs affects the deviation in points detected around that region. Another reason is that the length of the horse in the Figure 5.2a is smaller than that in the Figure 5.2b which leads to deviation in the buttock point detection.

The possible solution for this is to create an algorithm to detect points based on the length of the horse, which would help in better identifying the range that needs to selected from the extreme points. Another possible solution for the above problem is to train a deep learning based neural network [74] [75] [76] to detect the key points of a horse. This would require a well labelled dataset of good conformation horses from a horse breeder.

5.3.2 Colour of the Horse

The colour analysis of a horse as presented in the Section 3.3.4 uses Kmeans clustering algorithm for segregating the colours of the horse. This helps in determining the presence of joint angles because when seen from a naked eye, the area around joints of the horse appears to be little darker in shade. This fails for white coloured horses because of the insignificant difference in the colour shade around the joint angles. Figure 5.3 shows that the horse image does not show any significant change in colour around the joint angles.

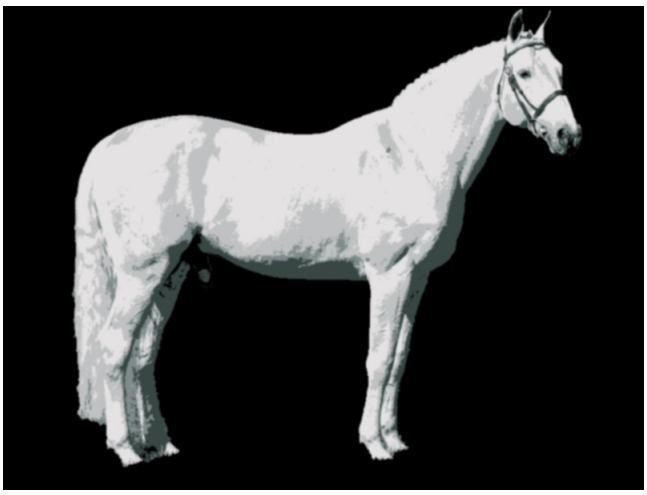

Figure 5.3: The result of colour analysis performed over white coloured horse. It does not show any significant finding for the joint angles around hip region.

A possible solution for this is presented in the study [77] where colour based clustering and segmentation is performed using Neural Networks. In this study both supervised learning method and unsupervised learning method was used for colour clustering.

Chapter 6

Conclusion and Future Work

6.1 Conclusion

This dissertation explores the possibility of automated analysis of horse conformation in order to determine the calibre of the horse. This would reduce the time and effort of a horse buyer to get the conformation of horse analysed from a horse expert or breeder before buying.

The results obtained in the Section 5.2 gives a confidence that the algorithm developed was capable in analysing the conformation of a horse and deciding whether the horse is Good Balanced or not. While there were some deviations observed in few images due to the varying shape and stance of the horse, the thesis lays a solid foundation for further improving or fine tuning the algorithm.

The following conclusions were made based on the results obtained by this research:

- An algorithm could be created to segregate the horse image from the background. This research uses a combination of Deep Learning based pre-trained model to generate a mask of the horse, colour segment the mask using the HSV channels and then finally extract the horse.
- Colour and Texture Analysis could be used for visual verification of the angular proportions calculated.
- An algorithm could be created based on the extreme left, right, top, bottom and

center of gravity points, to detect the key points located around the edges of the horse.

The study of horse conformation is a vast research subject and the research shows some of the limitations of the algorithm along with a possible solution for the same. To sum up, the research has shown feasibility that it can be used on a 2D equine image to automatically analyse the Good Balance of a horse.

6.2 Future Work

It is evident from the limitations of the research that there is a scope for improvement in this. The study of horse conformation is a vast research subject and there are many other aspects of a horse that could be analysed to better evaluate the conformation of a horse.

- A larger dataset with conformation labelled via an expert can help in building a CNN Fuzzy fusion or supervised machine learning approach for detecting the points of interest on the horse.
- A larger horse image dataset could be used to create deep learning based R-CNN, Faster-CNN model for foreground extraction, reducing the number of steps used in the research, thus saving time and memory.
- Analysis of front and back profile of the horse, i.e. entire 3D structure of the horse could also be carried out to determine the Structural correctness of a horse.
- Streamlining this project for future use would also allow for it to more easily be converted to a mobile application by deploying the algorithm over some cloud server like AWS, and then capturing a horse image from mobile and passing it onto the algorithm could send the conformation score in response.
- The research methodologies could also help in building something similar for Camel Conformation, which is another huge industry in the Arabian countries.
- The research could also be extended further to identify the muscle mass properties and sex/breed characteristics of a cattle, which could be beneficial is analysing the cattle's value before importing/exporting them to/from third world countries.

Bibliography

[1] C. S. Cable, "Conformation in horses - the horse." Available at https://thehorse.com/14024/conformation-in-horses/. [Accessed: 27-Aug-2020].

[2] A. I. Gmel, T. Druml, R. von Niederhäusern, T. Leeb, and M. Neuditschko, "Genome-wide association studies based on equine joint angle measurements reveal new qtl affecting the conformation of horses," *Genes 2019*, vol. 370, 2019.

[3] K. J. Duberstein, "Evaluating horse conformation." University of Georgia Cooperative Extension, 2016.

[4] *Conformation*. WP and CS of Australia Inc. Handbook, 2013.

[5] A. I. Gmel, T. Druml, R. von Niederhäusern, T. Leeb, and M. Neuditschko, "Repeatability, reproducibility and consistency of horse shape data and its association with linearly described conformation traits in franches-montagnes stallions," 2018.

[6] M. Ryan, "Analysing equestrian images in order to determine quality and calibre of a horse." BSc International Computational Thinking, Maynooth University, 2019.

[7] C. H. Chen, "An automatic equine conformation rating system using digital image processing," Master's thesis. MSc in Computer Science, Maynooth University, 2019.

[8] M. J. Arns, *Kansas Youth Horse Judging Manual*. Kansas State University.

[9] W. Loch, "Horses - conformation: Form to function." Available at https://extension2.missouri.edu/g2837/. [Accessed: 27-Aug-2020].

[10] *4-H Horse Judging Manual*. Washington State University.

[11] J. Timoney, B. Faghih, and W. M. Carter, "Automatic horse conformance," *IEEE Transactions on Neural Networks*, vol. 16 - No.4, 2019.

[12] "Opencv computer vision library." Available at https://opencv.org/. [Accessed: 27-Aug-2020].

[13] "Interactive foreground extraction using grabcut algorithm." Available at https://docs.opencv.org/3.4/d8/d83/tutorial_py_grabcut.html. [Accessed: 27-Aug-2020].

[14] "Canny edge detection." Available at https://docs.opencv.org/trunk/da/d22/tutorial_py_canny.html. [Accessed: 27-Aug-2020].

[15] "Harris corner detector." Available at https://docs.opencv.org/3.4/d4/d7d/tutorial_harris_detector.html. [Accessed: 27-Aug-2020].

[16] T. Druml, M. Dobretsberger, and G. Brem, "Ratings of equine conformation – new insights provided by shape analysis using the example of lipizzan stallions," *Archives Animal Breeding*, vol. 309-317, 2016.

[17] T. Druml, M. Dobretsberger, and G. Brem, "The use of novel phenotyping methods for validation of equine conformation scoring results," *The Animal Consortium*, vol. 9:6, 2015.

[18] "Global horse racing market 2019 is set to be a billion dollar industry by 2026 according to market forecasts – mrs research group." Available at https://www.globenewswire.com/news-release/. [Accessed: 27-Aug-2020].

[19] "Horse industry generates $122 billion economic impact." Available at https://www.quarterhorsenews.com/. [Accessed: 27-Aug-2020].

[20] A. Rosebrock, "Finding extreme points in contours with opencv." Available at https://www.pyimagesearch.com/2016/04/11/finding-extreme-points-in-contours-with-opencv/. [Accessed: 27-Aug-2020].

[21] A. Rosebrock, "Keras mask r-cnn." Available at https://www.pyimagesearch.com/2019/06/10/keras-mask-r-cnn/. [Accessed: 27-Aug-2020].

[22] "Image segmentation using color spaces in opencv + python." Available at https://realpython.com/python-opencv-color-spaces/. [Accessed: 27-Aug-2020].

[23] A. Rosebrock, "Holistically-nested edge detection with opencv and deep learning." Available at https://www.pyimagesearch.com/2019/03/04/holistically-nested-edge-detection-with-opencv-and-deep-learning/. [Accessed: 27-Aug-2020].

[24] "K-means clustering in opencv." Available at https://docs.opencv.org/master/d1/d5c/tutorial_py_kmeans_opencv.html. [Accessed: 27-Aug-2020].

[25] A. Rosebrock, "Local binary patterns with python & opencv." Available at https://www.pyimagesearch.com/2015/12/07/local-binary-patterns-with-python-opencv/. [Accessed: 27-Aug-2020].

[26] "Smoothing images." Available at https://docs.opencv.org/master/d4/d13/tutorial_py_filtering.html. [Accessed: 27-Aug-2020].

[27] "Shi-tomasi corner detector." Available at https://docs.opencv.org/3.4/d8/dd8/tutorial_good_features_to_track.html. [Accessed: 27-Aug-2020].

[28] "Stallion selection: Horse sport ireland." Available at https://www.horsesportireland.ie/breeding/stallion-selections/. [Accessed: 27-Aug-2020].

[29] N. Ellis, "The importance of good conformation in horses." Available at https://horsesandfoals.com/horse-conformation/. [Accessed: 27-Aug-2020].

[30] C. Corp-Minamiji, "The importance of limb conformation." Available at https://thehorse.com/. [Accessed: 27-Aug-2020].

[31] "Equine conformation – the key to soundness: Ashbrook equine hospital." Available at https://www.wikipet.co.uk/pet-health/2998/. [Accessed: 27-Aug-2020].

[32] H. S. Thomas, "The importance of conformation when selecting a horse." Available at https://equimed.com/health-centers/lameness/articles/the-importance-of-conformation-when-selecting-a-horse/. [Accessed: 27-Aug-2020].

[33] T. Kristjansson, S. Bjornsdottir, E. Albertsdóttir, A. Sigurdsson, P.Pourcelot, N.Crevier-Denoix, and T. Arnason, "Association of conformation and riding ability in icelandic horses," *Livestock Science*, vol. 189, 2016.

[34] H. Ghezelsoflou, P. Hamidi, and S. Gharahveysi, "Study of factors affecting the body conformation traits of iranian turkoman horses," *Japanese Society of Equine Science*, vol. 29 - No.4, 2018.

[35] "Breeding policy." Available at https://www.horsesportireland.ie/breeding/breeding-policy/. [Accessed: 27-Aug-2020].

[36] R. Girshick, J. Donahue, T. Darrell, and J. Malik, "Rich feature hierarchies for accurate object detection and semantic segmentation," 2014.

[37] A. Rosebrock, "Region proposal object detection with opencv, keras, and tensorflow." Available at https://www.pyimagesearch.com/2020/07/06/region-proposal-object-detection-with-opencv-keras-and-tensorflow/. [Accessed: 27-Aug-2020].

[38] A. G. Howard, M. Zhu, B. Chen, D. Kalenichenko, W. Wang, T. Weyand, M. Andreetto, and H. Adam, "Mobilenets: Efficient convolutional neural networks for mobile vision applications," 2017.

[39] A. Malhotra, "Car image segmentation using convolutional neural nets." Available at https://medium.com/weightsandbiases/car-image-segmentation-using-convolutional-neural-nets-7642448028f6. [Accessed: 27-Aug-2020].

[40] A. Rosebrock, "Instance segmentation with opencv." Available at https://www.pyimagesearch.com/2018/11/26/instance-segmentation-with-opencv/. [Accessed: 27-Aug-2020].

[41] K. He, G. Gkioxari, P. Dollár, and R. Girshick, "Mask r-cnn," 2018.

[42] P. A and S. Vas, "Edge detection using deep learning," *International Research Journal of Engineering and Technology*, vol. 05, 2018.

[43] Y. Liu1, M.-M. Cheng, D.-P. Fan, L. Zhang, J.-W. Bian, and D. Tao, "Semantic edge detection with diverse deep supervision," *International Journal of Computer Vision*, 2020.

[44] P. Dollar, Z. Tu, and S. Belongie, "Supervised learning of edges and object boundaries,"

[45] M. A. El-Sayed, "Edge detection using convolutional neural network," *International Journal of Advanced Computer Science and Applications*, vol. 4, 2013.

[46] S. Xie and Z. Tu, "Holistically-nested edge detection," *Computer Vision and Pattern Recognition*, 2015.

[47] A. Z. Chitade and D. S. Katiyar, "Colour based image segmentation using k-means clustering," *International Journal of Engineering Science and Technology*, vol. 2(10), 2010.

[48] A. Mohanty, S. Rajkumar, Z. M. Mir, and P. Bardhan, "Analysis of color images using cluster based segmentation techniques," *International Journal of Computer Applications*, vol. 79 - No.2, 2019.

[49] G. Mathur and D. H. Purohit, "Performance analysis of color image segmentation using k-means clustering algorithm in different color spaces," *IOSR Journal of VLSI and Signal Processing*, vol. 4, Issue 6, 2014.

[50] J. Huang, J. Zhao, W. Gao, C. Long, L. Xiong, Z. Yuan, and S. Han, "Local binary pattern based texture analysis for visual fire recognition," *3rd International Congress on Image and Signal Processing*, 2010.

[51] T. Ojala, M. Pietikäinen, and T. Mäenpää, "Multiresolution gray scale and rotation invariant texture classification with local binary patterns,"

[52] R. Girshick, J. Donahue, T. Darrell, and J. Malik, "Rich feature hierarchies for accurate object detection and semantic segmentation," 2014.

[53] R. Girshick, "Fast r-cnn," 2015.

[54] S. Ren, K. He, R. Girshick, and J. Sun, "Faster r-cnn: Towards real-time object detection with region proposal networks," 2016.

[55] I. Matterport, "Mask r-cnn pre-trained model." Available at https://github.com/matterport/Mask_RCNN. [Accessed: 27-Aug-2020].

[56] C. Commons, "Coco dataset." Available at https://cocodataset.org/#home. [Accessed: 27-Aug-2020].

[57] C. Rother, V. Kolmogorov, and A. Blake, ""grabcut" — interactive foreground extraction using iterated graph cuts." Available at https://cvg.ethz.ch/teaching/cvl/2012/grabcut-siggraph04.pdf. [Accessed: 27-Aug-2020].

[58] A. Rosebrock, "Opencv grabcut: Foreground segmentation and extraction." Available at https://www.pyimagesearch.com/2020/07/27/opencv-grabcut-foreground-segmentation-and-extraction/. [Accessed: 27-Aug-2020].

[59] P. Patidar and S. Srivastava, "Image de-noising by various filters for different noise," *International Journal of Computer Applications*, vol. 9- No.4, 2010.

[60] O. R. Systems. Available at https://www.theobjects.com/dragonfly/dfhelp/30/Content/07_Image%20Processing/Smoothing%20Filters.htm. [Accessed: 27-Aug-2020].

[61] M. Celenk, "A color clustering technique for image segmentation," *Computer Vision, Graphics, and Image Processing*, vol. 52, Issue 2, 2004.

[62] P. Sharma, "Computer vision tutorial: A step-by-step introduction to image segmentation techniques." Available at https://www.analyticsvidhya.com/blog/2019/04/introduction-image-segmentation-techniques-python/. [Accessed: 27-Aug-2020].

[63] "Scikit image." Available at https://scikit-image.org/. [Accessed: 27-Aug-2020].

[64] "Deep learning based edge detection in opencv." Available at https://cv-tricks.com/opencv-dnn/edge-detection-hed. [Accessed: 27-Aug-2020].

[65] "Nyu depth." Available at https://cs.nyu.edu/~silberman/datasets/. [Accessed: 27-Aug-2020].

[66] "The berkeley segmentation dataset and benchmark." Available at https://www2.eecs.berkeley.edu/Research/Projects/CS/vision/bsds/. [Accessed: 27-Aug-2020].

[67] "Corner detection: Harris corner and shi-tomasi corner detection." Available at https://www.programmersought.com/article/2622158355/. [Accessed: 27-Aug-2020].

[68] Shi and C. Tomasi, "Good features to track," *Proceedings of the IEEE Conference on Computer Vision and Pattern Recognition*, 1994.

[69] H. A.Kadhima and W. A.Araheemah, "A comparative between corner-detectors (harris, shi-tomasi & fast) in images noisy using non-local means filter," *Journal of Al-Qadisiyah for Computer Science and Mathematics*, vol. 11(3), 2019.

[70] N. Gandhi, "Harris corner detection and shi-tomasi corner detection." Available at https://medium.com/pixel-wise/detect-those-corners-aba0f034078b. [Accessed: 27-Aug-2020].

[71] A. Rosebrock, "Opencv center of contour." Available at https://www.pyimagesearch.com/2016/02/01/opencv-center-of-contour/. [Accessed: 27-Aug-2020].

[72] E. Furey, "Two dimensional distance calculator." Available at https://www.calculatorsoup.com/calculators/geometry-plane/distance-two-points.php. [Accessed: 27-Aug-2020].

[73] M. Murugavel, "Find the angle between three points from 2d using python." Available at https://medium.com/@manivannan_data/find-the-angle-between-three-points-from-2d-using-python-348c513e2cd. [Accessed: 27-Aug-2020].

[74] P. L. Liu, "Self-supervised keypoint learning — a review." Available at https://towardsdatascience.com/self-supervised-keypoint-learning-aade18081fc3. [Accessed: 27-Aug-2020].

[75] H. Altwaijry, A. Veit, and S. Belongie, "Learning to detect and match keypoints with deep architectures," *British Machine Vision Conference*, 2016.

[76] D. DeTone, T. Malisiewicz, and A. Rabinovich, "Superpoint: Self-supervised interest point detection and description," 2018.

[77] G. Dong and M. Xie, "Color clustering and learning for imagesegmentation based on neural networks," *IEEE Transactions on Neural Networks*, vol. 16 - No.4, 2005.

Appendix A

gender:			name:									
height at withers:			reg. no.:							cat. no.:		
markings:			sire:							dam:		
markings not allowed:			reg. no.:							reg. no.:		
judging location:			date:							jury member:		
element	characteristic	groep	5	10	15	20	25	30	35	40	45	characteristic
head	plain	racial										noble
head-neck connection	heavy	frame										light
neck	short	rac/frame										long
	horizontal	racial										vertical
shoulder	steep	frame										sloping
back	weak	frame										tight
loins	weak	frame										tight
croup	straight	frame										sloping
	short	frame										long
body	downhill	frame										upstanding
length forearm	short	frame										long
frontlegs	straight	feet&legs										standing under
hindlegs	sickled	feet&legs										straight
pasterns	short	feet&legs										long
hooves	small	feet&legs										large
quality of legs	course	feet&legs										hard
hair	little	racial										much
color	faded black	racial										jet black
frontlegs	toeing-in	feet&legs										toeing-out
walk	short	walk										long
	weak	walk										powerful
trot	short	trot										long
	weak	trot										powerful
	unbalanced	trot										balanced
	not supple	trot										supple
	racialtype	frame	feet & legs		walk		trot					

Figure A.1: Example of a Linear Scoring Form

Appendix B

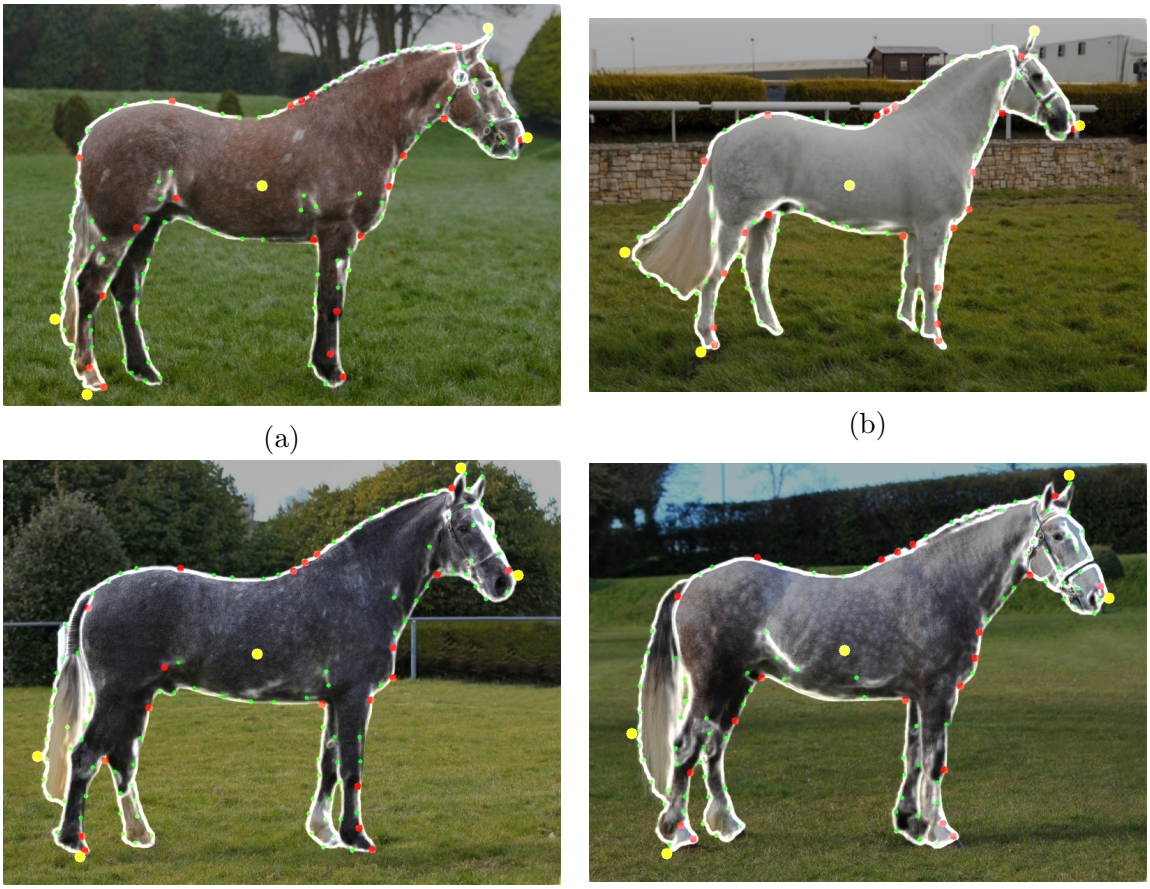

(a) (b)

(c) (d)

Figure B.1: An example illustration of good conformation results obtained irrespective of the colour of the horse. The conformation score for these horses are **(a), (b), (c), (d) : (20/23, 18/23, 18/23, 19/23)**. The difference in the height of the images is because the images were resized using the scale factor set to width = 800.

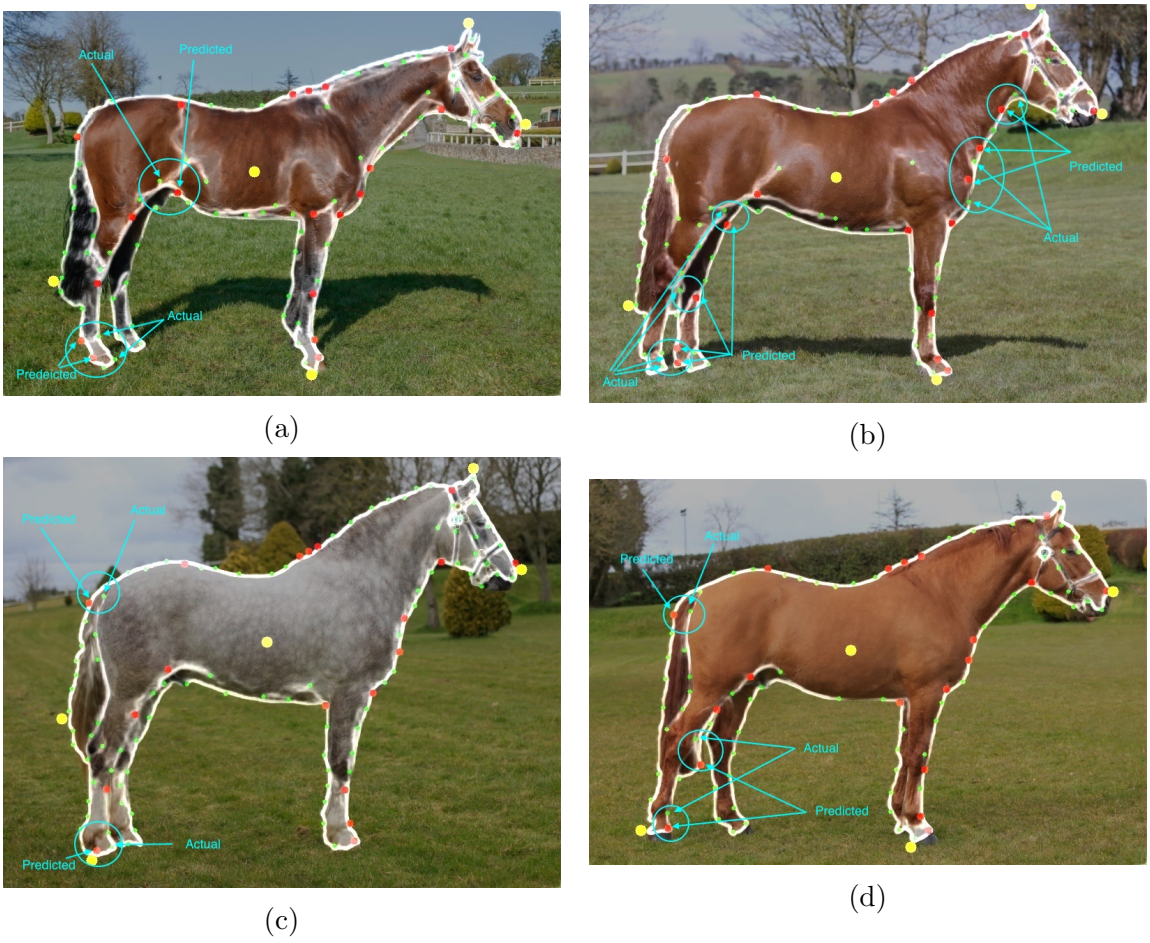

Figure B.2: An example illustration of measure of error displacement if the key point detection of the horse. The conformation score obtained for these horses are **(a), (b), (c), (d) : (21/23, 18/23, 20/23, 19/23)**. The difference in the height of the images is because the images were resized using the scale factor set to width = 800.